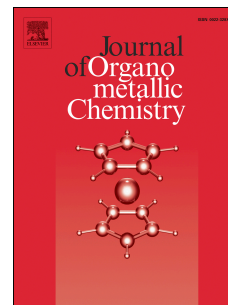


Accepted Manuscript

Synthesis and Reactivity of Bis(diphenylphosphino)amine-bridged Heterobimetallic Iron-Platinum μ -Isonitrile and μ -Aminocarbyne Complexes

Michael Knorr, Isabelle Jourdain, Ahmed Said Mohamed, Abderrahim Khatyr, Stephan Koller, Carsten Strohmann



PII: S0022-328X(14)00630-5

DOI: [10.1016/j.jorganchem.2014.12.028](https://doi.org/10.1016/j.jorganchem.2014.12.028)

Reference: JOM 18853

To appear in: *Journal of Organometallic Chemistry*

Received Date: 15 November 2014

Revised Date: 15 December 2014

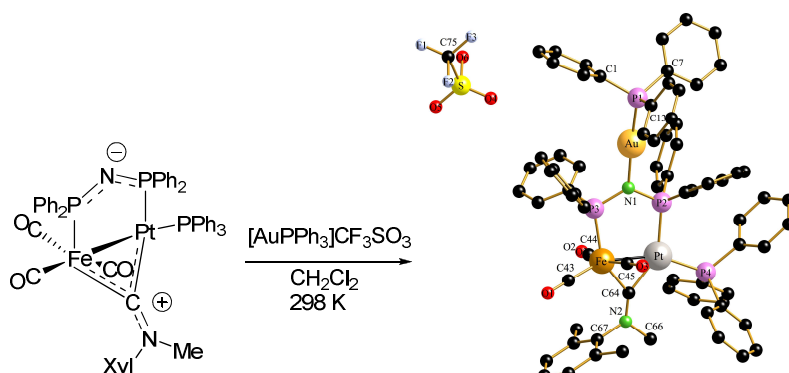
Accepted Date: 19 December 2014

Please cite this article as: M. Knorr, I. Jourdain, A.S. Mohamed, A. Khatyr, S. Koller, C. Strohmann, Synthesis and Reactivity of Bis(diphenylphosphino)amine-bridged Heterobimetallic Iron-Platinum μ -Isonitrile and μ -Aminocarbyne Complexes, *Journal of Organometallic Chemistry* (2015), doi: 10.1016/j.jorganchem.2014.12.028.

This is a PDF file of an unedited manuscript that has been accepted for publication. As a service to our customers we are providing this early version of the manuscript. The manuscript will undergo copyediting, typesetting, and review of the resulting proof before it is published in its final form. Please note that during the production process errors may be discovered which could affect the content, and all legal disclaimers that apply to the journal pertain.

Graphical abstract

Zwitterionic heterobimetallic aminocarbonyl complexes $[(OC)_2(L)Fe\{\mu-CN(R)R'\}\{\mu-Ph_2PNPPh_2\}Pt(PPh_3)]$ ($L = CO, CNR$) have been synthesized by deprotonation of the bridging dppa ligand and their reactivity towards various electrophiles has been investigated. Thus, *N*-alkylated or *N*-metallated aminocarbonyl complexes such as the heterotrimeric gold-amide complex $[(OC)_3Fe\{\mu-CN(Me)xyl\}\{\mu-Ph_2PN(AuPPh_3)PPh_2\}Pt(PPh_3)][OSO_2CF_3]$ have been obtained.

**Highlights**

- Heterobimetallic isonitrile and μ -aminocarbonyl Fe-Pt complexes have been synthesized.
- The bonding mode of the CNR ligand (bridging vs. terminal) depends on the σ -donor/ π -acceptor propensity of R.
- Regioselective substitution of PPh_3 at the Pt center.
- Zwitterionic compounds were obtained by deprotonation of the dppa ligand.
- Heterotrimeric aminocarbonyls were characterized by multinuclear NMR and X-ray diffraction.

Heterobimetallic Iron-Platinum μ -Isonitrile and μ -Aminocarbyne Complexes

Michael Knorr* ^[a], Isabelle Jourdain* ^[a], Ahmed Said Mohamed, ^[a] Abderrahim Khatyr ^[a], Stephan Koller ^[b], Carsten Strohmann ^[b]

Dedicated to Prof. Jacques Amaudrut on the occasion of his 75th birthday

^a Institut UTINAM UMR CNRS 6213, Université de Franche-Comté,

Faculté des Sciences et des Techniques, 16, Route de Gray, 25030 Besançon, France

^b Institut für Anorganische Chemie der Technischen Universität Dortmund, Otto-Hahn-Strasse 6, 44227 Dortmund, Germany

ABSTRACT

Reaction of $[(OC)_3Fe(\mu-CO)(\mu-dppa)Pt(PPh_3)]$ (**1**) (dppa = bis(diphenylphosphino)amine) with various isonitriles in a 1:1 or 1:2 ratio yields the isonitrile-bridged compounds $[(OC)_3Fe(\mu-CN-R)(\mu-dppa)Pt(PPh_3)]$ (**2**) and $[(OC)_2(RNC)Fe(\mu-CN-R)(\mu-dppa)Pt(PPh_3)]$ (**3**), respectively. However, addition of *tert*-butylisonitrile to **1** affords the carbonyl-bridged complex $[(OC)_2(tert-BuNC)Fe(\mu-CO)(\mu-dppa)Pt(PPh_3)]$ (**2g**). Upon treatment of $[(OC)_3Fe(\mu-CN-o-anisyl)(\mu-dppa)Pt(PPh_3)]$ (**2b**) with SO₂, the μ -CNR ligand is chased from its bridging position to give the sulfur dioxide-bridged compound $[(OC)_2(o-anisylNC)Fe(\mu-SO_2)(\mu-dppa)Pt(PPh_3)]$ (**4**). These compounds are converted to the μ -aminocarbyne salts $[(OC)_2(L)Fe\{\mu-CN(R)R'\}(\mu-dppa)Pt(PPh_3)]^+$ (**5** R' = Me, Et) by *N*-alkylation using [Me₃O][BF₄] or ethyl triflate as electrophiles. In function of the sterical crowding exerted by μ -aminocarbyne groups, two stereoisomers can be formed. Upon addition of P(OMe)₃ or *tert*-BuNC to **5**, no carbonyl substitution occurs. Instead the Pt-bound PPh₃ ligand is replaced by L' in a regioselective manner to give $[(OC)_2(L)Fe\{\mu-CN(Me)R\}(\mu-dppa)Pt(L')][BF_4]$ (**5e**, **5f**, **5g**). Deprotonation of the N-H function of the bis(diphenylphosphino)amine ligand of salts **5** by KSi(OMe)₃ or KH produces the zwitterionic compounds $[(OC)_2(L)Fe\{\mu-CN(R)R'\}(\mu-Ph_2PNPPh_2)Pt(PPh_3)]$ (**6**). The latter react with various organic and inorganic electrophiles to produce the *N*-alkylated or metallated aminocarbyne complexes $[(OC)_2(L)Fe\{\mu-CN(R)R'\}\{\mu-Ph_2PN(E)PPh_2\}Pt(PPh_3)]^+$ (**7**: E = Me, **8**: E = AuPPh₃, CuAsPh₃, CuPPh₃, HgMe). The molecular structures of **2c**, **3b**, **5b**, **8a** and **8b** have been determined by X-ray diffraction studies.

Keywords: Heterobimetallic complexes / Isonitrile complexes / Aminocarbyne complexes / Iron / Platinum

1. Introduction

The use of bis(diphenylphosphino)methane (dppm) as short-bite ligand to assemble homo- and heterodinuclear complexes is documented in a plethora of articles and even some reviews deal on the coordination chemistry of dppm [1]. Although the first examples on the use of the related ligand bis(diphenylphosphino)amine (dppa) have been reported in the seventies, [2] considerably less work on the synthesis and reactivity of heterodinuclear and heterotrinnuclear systems spanned by dppa are documented. Some selected examples are $[(OC)_3Mo(\mu-dppa)_2RhCl(CO)]$ [3], $[(C_6F_5)_2Pd(\mu-dppa)_2Ag][ClO_4]$ [4], $[(OC)_4Fe(\mu-dppa)ReBr(CO)_4]$ [5a], $[(OC)_3Fe\{\mu-Si(OMe)_2(OMe)\}(\mu-dppa)Pd(I)]$ [5b], $[(OC)_4Fe(\mu-dppa)Pd(CH_2CH_2C(=O)Me)][BF_4]$ [5c], $[Cp(PPh_3)RuCl(\mu-dppa)AuCl]$ [6], $[(OC)_3Fe(\mu-dppa)\{\mu-C(C_6H_4CF_3-o)C=C(H)\}Pt(PPh_3)]$ [7], $[(Cp)Ru(\mu-CO)_2(\mu-dppa)MCl_2]$ (M = Rh, Ir) [8], and $[Cp(OC)_2Mo(\mu-dppa)Pt(CO)Mo(CO)_3Cp]$ [10]. With the objective to combine our research interest on heterobimetallic complexes bearing bridging isonitrile ligands, we have reported several years ago on the synthesis of the carbonyl-bridged complex $[(OC)_3Fe(\mu-C=O)(\mu-dppa)Pt(PPh_3)]$ (**1**) and its reactivity towards aromatic isonitriles leading to a series of $[(OC)_3Fe(\mu-CN-Ar)(\mu-dppa)Pt(PPh_3)]$ complexes [11]. We have also demonstrated that the latter can be converted to cationic aminocarbyne complexes $[(OC)_3Fe\{\mu-C=N(E)Ar\}(\mu-dppa)Pt(PPh_3)]^+$ by addition of electrophiles E on the basic N-atom of the bridging isonitrile ligand. Since heterometallic μ -aminocarbyne complexes are still very scarce, we have since our first short report investigated more in detail the synthetic access, structural features and reactivity of this species. Another objective of this paper is the exploration of the possibility to use the presence of the dppa-bridge to construct heterotrimetallic aminocarbyne complexes. The synthesis of these heterotrimetallic systems, their characterisation by multinuclear NMR studies and X-ray diffraction is presented in the second part of this article.

2. Results and Discussion

2.1. Synthesis of Fe-Pt Mono- and Bis(isonitrile) Complexes

In a manner similar as already described for the preparation of complexes $[(OC)_3Fe(\mu-CN-xylyl)(\mu-dppa)Pt(PPh_3)]$ (**2a**) and $[(OC)_3Fe(\mu-CN-o-anisyl)(\mu-dppa)Pt(PPh_3)]$ (**2b**), [11] reaction of $[(OC)_3Fe(\mu-CO)(\mu-dppa)Pt(PPh_3)]$ (**1**) with the aliphatic benzylisonitrile in a 1:1 ratio gives cleanly within 10 min the isonitrile-bridged compound $[(OC)_3Fe(\mu-CN-benzyl)(\mu-dppa)Pt(PPh_3)]$ (**2c**), isolated in 88% yield (Scheme 1). The isonitrile ligand adopts also a bridging bonding mode after

stoichiometric addition of isocyanomethylacetate and *p*-tosylmethylisonitrile affording $[(\text{CO})_3\text{Fe}\{\mu\text{-CN-CH}_2\text{C(=O)OMe}\}(\mu\text{-dppa})\text{Pt}(\text{PPh}_3)]$ (**2d**) and $[(\text{CO})_3\text{Fe}\{\mu\text{-CN-CH}_2\text{SO}_2\text{p-Tol}\}(\mu\text{-dppa})\text{Pt}(\text{PPh}_3)]$ (**2e**), respectively. The crystal structure of **2c** is shown in the Supporting Information (Figure S1). Exemplarily for these series **2**, the $^{31}\text{P}\{^1\text{H}\}$ NMR spectrum of **2e** is depicted in Figure 1, the NMR data for all complexes are presented in Table 3.

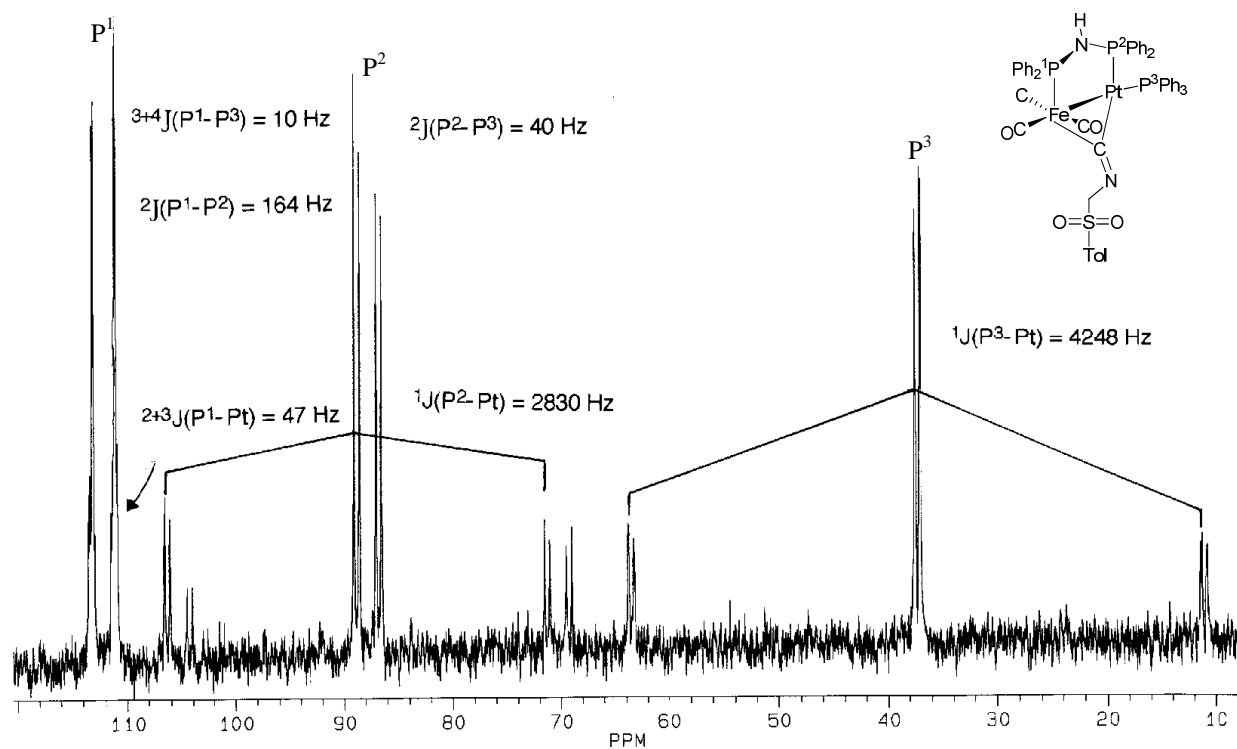
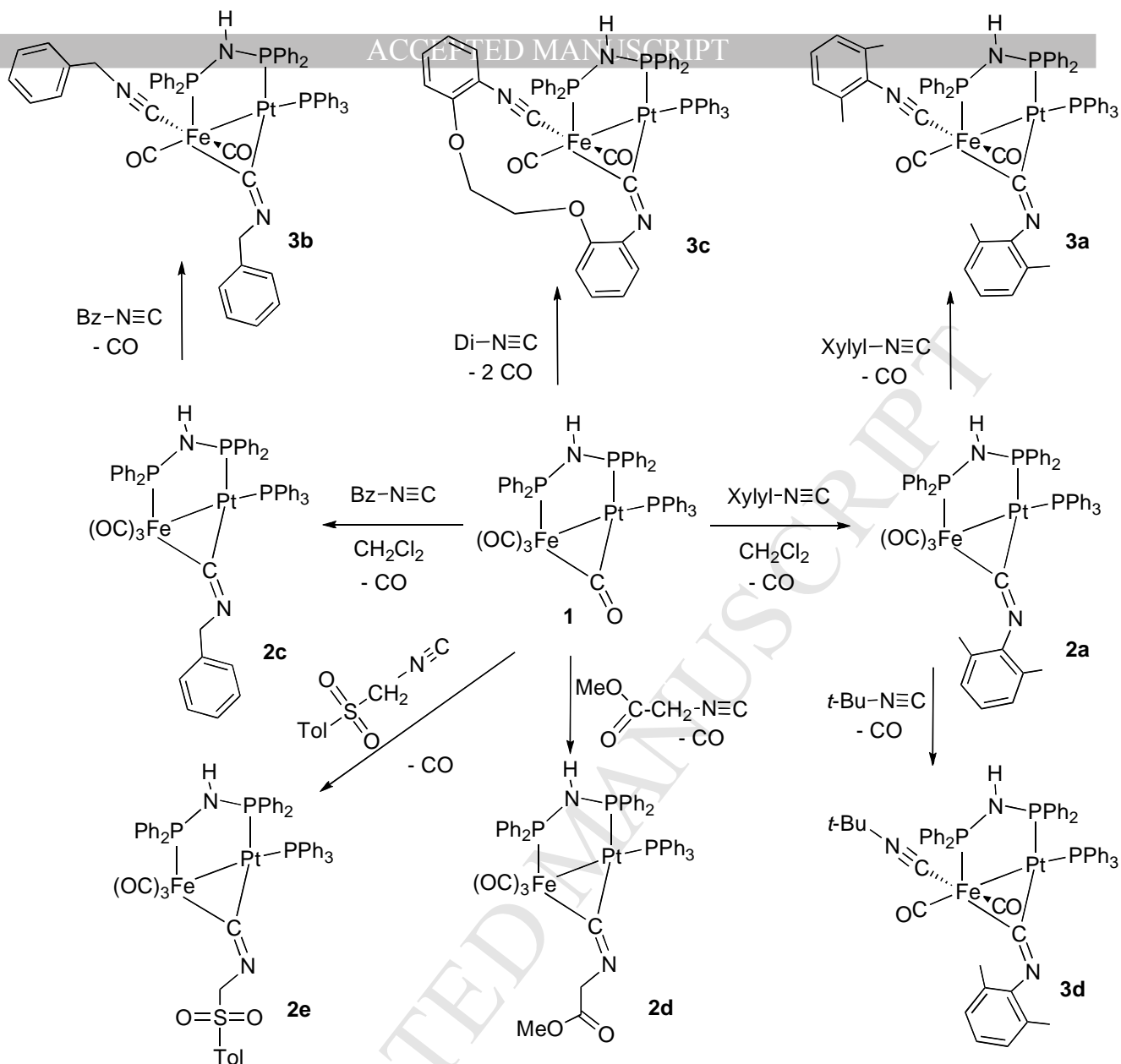


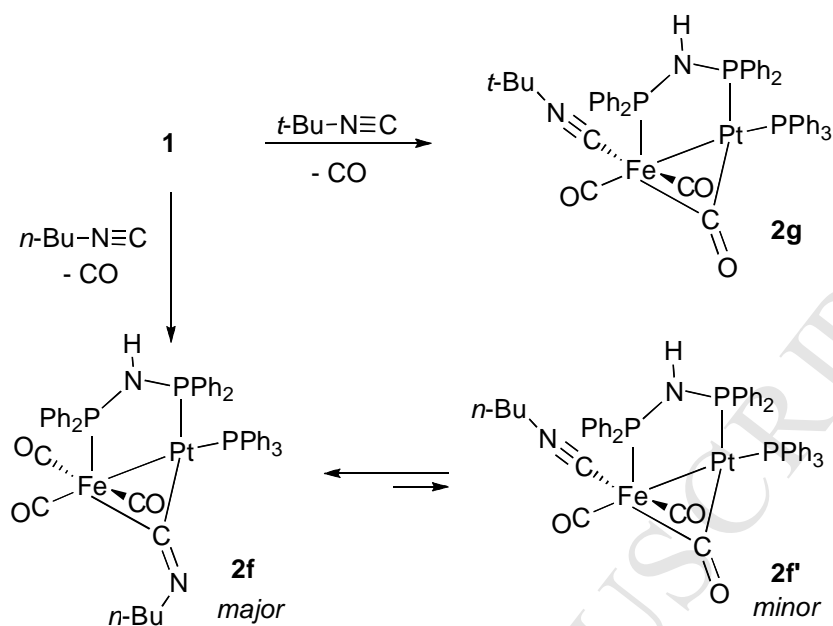
Fig. 1. $^{31}\text{P}\{^1\text{H}\}$ NMR spectrum of **2e** recorded in CDCl_3 at 298 K.



Scheme 1. Syntheses of heterodinuclear mono- and bis(isonitrile) complexes

The reaction becomes more complicated when using stronger electron-donating aliphatic isocyanides. Addition of *n*-butylisonitrile to **1** produces in almost quantitative yield the substitution product $[(\text{CO})_3\text{Fe}(\mu\text{-CN-Bu-}n)(\mu\text{-dppa})\text{Pt}(\text{PPh}_3)]$ (**2f**), which has been isolated as a yellow solid. The ^{31}P NMR spectrum recorded at 243 K exhibits chemical shifts and coupling constants quite comparable with those of **2e** illustrated in Figure 1. However, at 298 K two species are detectable in an approximate 60:40 ratio. The spectroscopic data of the first set correspond to those of the 243 K spectrum with a $^{2+3}J(\text{P-P})$ coupling of 180 Hz between the two dppa phosphorous atoms, the second set appears down-field shifted with respect to the first one with a $^{2+3}J(\text{P-P})$ coupling of 213 Hz. Overall the ^{31}P data of the second set are quite similar to those of the carbonyl-bridged precursor **1**. The IR spectrum in solution exhibits a broadened $\nu(\text{C=N})$ vibration at 1694 cm^{-1} stemming from the bridging isocyanide ligand, but there is also a further absorption at 2143 cm^{-1} characteristic for a

terminal isonitrile. We conclude that there is a temperature-dependent equilibrium between a μ -CNR isomer $[(\text{CO})_3\text{Fe}(\mu\text{-CN-Bu-}n)(\mu\text{-dppa})\text{Pt}(\text{PPh}_3)]$ (**2f**) and an isomeric μ -CO species **2f'** as shown in Scheme 2.



Scheme 2. Reactivity of **1** towards *n*-butyl and *t*-butyl isonitrile

This hypothesis is supported by the observation that after addition of a stoichiometric amount of *tert*-butylisonitrile the μ_2 -CO complex $[(\text{OC})_2(\text{tert-BuNC})\text{Fe}(\mu\text{-CO})(\mu\text{-dppa})\text{Pt}(\text{PPh}_3)]$ (**2g**) was formed. In this orange-colored microcrystalline solid, the isonitrile ligand adopts a terminal bonding mode orthogonal with respect to the Fe-Pt bond, which is bridged by a μ_2 -carbonyl ligand. The bonding situation is evidenced from the IR spectrum, which displays in addition to a broadened $\nu(\text{C}=\text{O})$ vibration at 1735 cm^{-1} an intense $\nu(\text{C}\equiv\text{N})$ absorption at 2123 cm^{-1} stemming from the terminal CNR ligand. The presence of two further strong $\nu(\text{CO})$ absorptions at 1950 and 1909 cm^{-1} proves that the CNR ligand is bound orthogonal to the metal-metal axis. In the alternative case of two *trans*-arranged terminal carbonyls only one band should have been observed. Compared to the position of $\nu(\text{C}=\text{O})$ band of precursor **1**, that of **2f** is shifted to lower frequency due to the electron-donating character of the *tert*-butylisonitrile ligand (1760 vs. 1735 cm^{-1}).

Of course the question arises, why *tert*-BuNC prefers to adopt a terminal bonding mode rather than a bridging one. A crystal structure of the first bimetallic example of a μ -CNR complex, $[\text{Cp}(\text{CO})\text{Fe}(\mu\text{-CNxylyl})(\mu\text{-CO})\text{FeCp}(\text{CO})]$, revealed a bridging bonding mode for xylylNC ligand (Chart 1) [12]. Some years later, Cotton and Adams studied the fluxional behavior of the *tert*-BuNC derivative and established crystallographically a terminal bonding mode for $[\text{Cp}(\text{CO})\text{Fe}(\text{tert-BuNC})(\mu\text{-CO})_2\text{FeCp}(\text{CO})]$ [13]. To explain this finding, the authors advanced steric arguments.

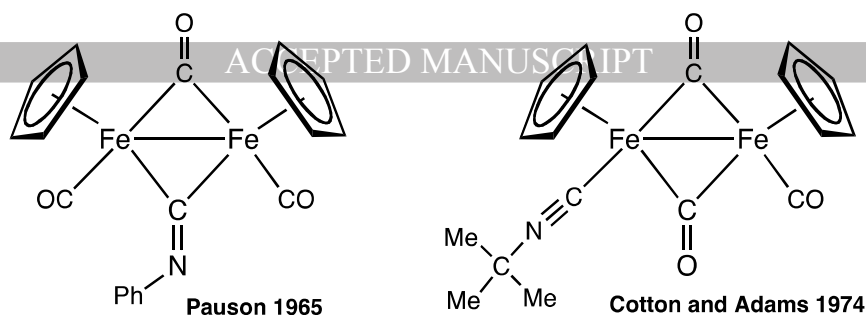


Chart 1

However, we are more in favor for a rationalization based on an electronic argumentation. In these electron-rich Fe-Pt complexes, a strong π -acceptor ligand such as μ -CO, μ -SO₂ (see below) or μ -CNR with aromatic or moderately electron-donating R group can compensate the electron-richness by back-bonding. However in the case of *tert*-BuNC, the strong electron-donating +I effect of the *t*-Bu group may considerably weaken the back-bonding propensity of this isocyanide, so that finally a μ -CO is more efficient as π -acceptor. Furthermore, our X-ray structure determination of the μ -vinylidene complex [(CO)₃Fe{ μ -C=C(H)*t*Bu}(μ -dppm)Pt(PPh₃)] demonstrates that a *t*-butyl group is able to adopt a bridging position without causing sterical hindrance [14].

Conducting the reaction of **1** in CH₂Cl₂ solution in the presence of 2 equivalents of RNC, or reacting **2a,c** with one further equivalent of RNC afforded the bis(isocyanide) complexes [(OC)₂(xylylINC)Fe(μ -CN-xylyl)(μ -dppa)Pt(PPh₃)] (**3a**) and [(OC)₂(BzNC)Fe(μ -CN-Bz)(μ -dppa)Pt(PPh₃)] (**3b**), respectively. Addition of the di(isocyanide) ligand 1,2-bis(2-isocyanophenoxy)ethane (diNC) to **1** results in formation of complex **3c**, in which one isocyanide group is bridging and the second one is ligated in a terminal manner on the iron center, thus forming a 13-membered macrocycle. We also succeeded to synthesize the mixed bis(isocyanide) complex [(OC)₂(*tert*-BuNC)Fe(μ -CN-xylyl)(μ -dppa)Pt(PPh₃)] (**3d**) by reacting **2a** with 1 equivalent of *tert*-BuNC. In the case of series **3**, the coordination of the terminal CNR ligand in an orthogonal position relative to the metal-metal bond can be deduced from the IR spectra, which shows two ν (CO) stretches of approximate equal intensities characteristic for a *cis*-arrangement of the two carbonyl ligands of the Fe(CO)₂ unit [15]. In addition, two ν (C \equiv N) vibrations due to the terminal and bridging isocyanide ligands are found in the IR spectra. For example, the terminal *tert*-BuNC ligand of **3d** gives rise to an adsorption at 2122 cm⁻¹, whereas the broadened band at 1652 cm⁻¹ is attributed to the bridging xylylINC ligand. Compared to complex **2a**, the position of the latter absorption is shifted to ca. 19 wavenumbers to lower frequencies. This is probably due to the additional electron donating effect of the second terminal CNR ligand, which is partially compensated by back-bonding in π^* -orbitals of the μ_2 -CNR ligand, thus weakening the C=N bond [16]. A ¹H NMR investigation of **3a** at variable temperature revealed the occurrence of a dynamic behavior of one xylylisonitrile ligand (Figure S2). At room temperature the methyl groups of each

xylylNC ligand appear as a singlet at δ 1.82 and 2.09, the later resonance being somewhat broadened. Progressive lowering of the temperature causes further broadening and coalescence is reached at 273 K. Below this temperature, a splitting of this signal occurs. Finally, two well-resolved singlets are observed at 243 K. We attribute these two singlets to the methyl groups of the bridging xylylNC ligand. Most probably, this phenomenon is a consequence of a hindered rotation around the Ar-N bond due to steric effect. An exchange between bridging and terminal CNR ligand has been discussed for other bimetallic systems [13] [17-21], but we exclude this possibility for **3a**, since the resonance due to the two methyl groups of the terminal xylylNC ligand are not involved in this dynamic behavior.

Crystal structure of [(CO)₂(BzNC)Fe(μ -CN-Bz)(μ -dppa)Pt(PPh₃)] (3b). The structural features, and selected bond length and angles of **3b** are presented in Figure 2. Suitable crystals of **3b**·0.5CH₂Cl₂ were grown from CH₂Cl₂/hexane. The structural parameters may be compared with those of the complex [(OC)₃Fe(μ -CN-Bz)(μ -dppa)Pt(PPh₃)] (**2c**) shown in Fig. S1. The replacement of one CO ligand by a second terminal xylylNC ligand hardly affects the Fe–Pt distance [2.5425(4) vs. 2.5741(13) Å]. The μ_2 -isonitrile ligand is symmetrically ligated between the two metal centers, the Fe–C(1) and Pt–C(1) distances being 2.000(9) and 1.998(10) Å. Both the length of the C(1)=N bond [1.259(12) vs. 1.233(3) Å] and the inclination C(1)–N–C(12) [120.8(9) vs. 122.2(2)°] correspond to that of **2c**. Also the bending of the benzyl group towards the carbonyl iron moiety is identical. The perpendicular disposition of the terminal benzylisonitrile deduced from the IR data is confirmed by this crystallographic study, the angle Pt–Fe–C(3) being 91.4(4)°. As expected for a terminal coordination, the C(3)–N(3)–C(4) array is almost linear (172.6(12)°), the presence of a C≡N triple bond is reflected by the short C(3)–N(3) distance of 1.175(15) Å.

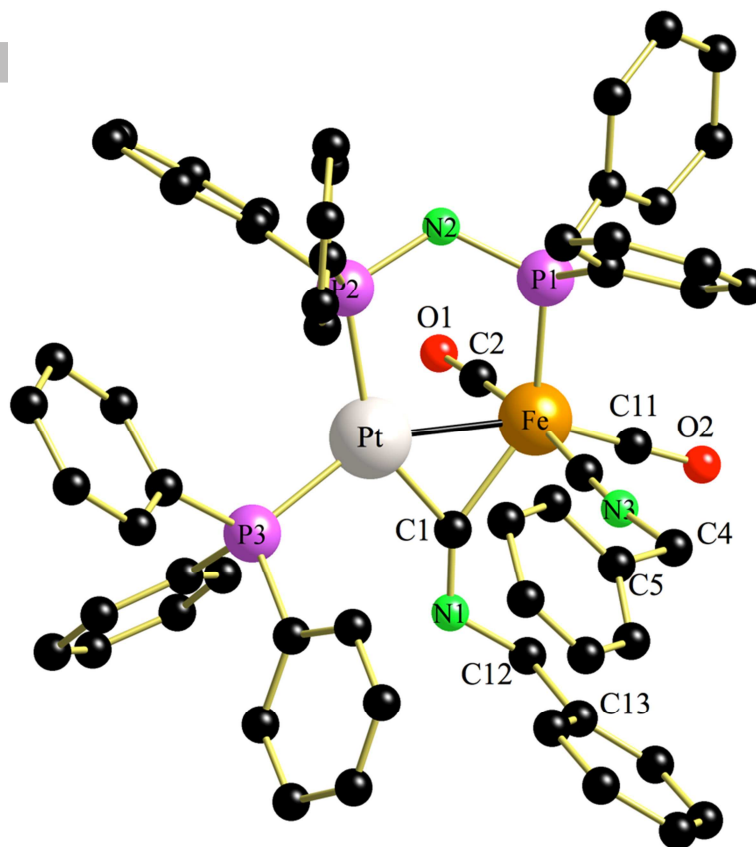
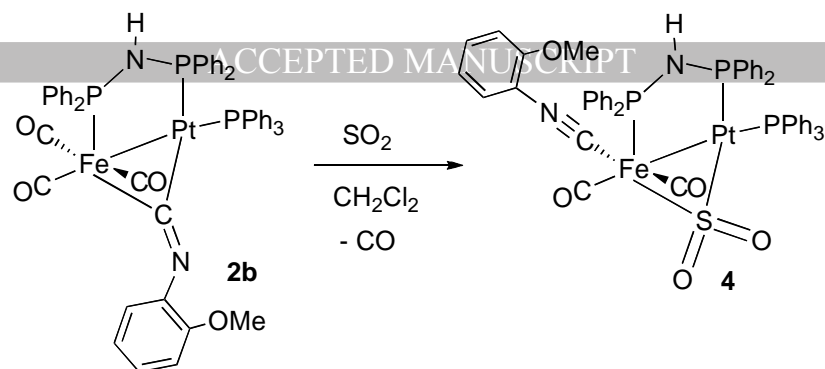


Fig. 2. Perspective view of **3b** showing the atom-labelling scheme. Hydrogen atoms and the CH₂Cl₂ molecule have been omitted for clarity. Selected distances (Å) and angles (°): Fe–Pt 2.5741(13), Fe–P(1) 2.228(2), Pt–P(2) 2.295(2), Pt–P(3) 2.269(2), Fe–C(1) 2.000(9), Fe–C(2) 1.713(11), Fe–C(3) 1.834(12), Fe–C(11) 1.730(11), Pt–C(1) 1.998(10), C(1)–N(1) 1.259(12), C(3)–N(3) 1.175(15), N(1)–C(12) 1.443(14), N(3)–C(4) 1.425(15), C(11)–O(2) 1.190(15), C(2)–O(1) 1.18(14), P(1)–N(2) 1.703(8), P(2)–N(2) 1.697(7); P(1)–Fe–Pt 91.33(7), P(2)–Pt–Fe 97.94(7), P(3)–Pt–Fe 148.58(7), P(3)–Pt–P(2) 113.36(8), Pt–C(1)–Fe 80.2(4), C(2)–Fe–Pt 83.2(4), C(11)–Fe–Pt 157.9(4), C(3)–Fe–Pt 91.4(4), C(1)–Pt–P(3) 99.0(3), C(1)–Pt–P(2) 147.6(3), C(1)–Fe–P(1) 140.7(3), N(3)–C(3)–Fe 176.5(11), C(3)–N(3)–C(4) 172.6(12), N(3)–C(4)–C(5) 111.9(11), P(1)–N(2)–P(2) 122.4(4), C(1)–N(1)–C(12) 120.8(9).

Table 1Crystallographic and refinement data for **3b**, **5b**, **5d** and **8a**

	3b •CH ₂ Cl ₂	5b	5d •CH ₂ Cl ₂ •Et ₂ O	8a
CCDC number	1031961	1031962	1031963	1031964
Formula	C ₁₂₁ H ₁₀₂ Cl ₂ Fe ₂ N ₆ O ₄ P ₆ Pt ₂	C ₅₄ H ₄₆ BF ₄ FeN ₂ O ₃ P ₃ Pt	C ₆₄ H ₆₉ BCl ₂ F ₄ FeN ₃ O ₃ P ₃ Pt	C ₇₄ H ₆₂ AuF ₃ FeN ₂ O ₆ P ₄ PtS
Formula weight [g·mol ⁻¹]	2462.69	1201.59	1429.78	1736.10
T [K]	173(2)	173(2)	293(2)	173(2)
Crystal size [mm]	0.20 x 0.10 x 0.10	0.30 x 0.20 x 0.20	0.30 x 0.20 x 0.20	0.30 x 0.20 x 0.10
Crystal system	orthorhombic	monoclinic	triclinic	monoclinic
Space group	<i>Pna</i> 2 ₁ (33)	<i>P</i> 2 ₁ / <i>c</i> (14)	<i>P</i> 1; ⁻ (2)	<i>P</i> 2 ₁ / <i>n</i> (14)
a [Å]	23.024(5)	11.732(2)	12.57(4)	16.8304(5)
b [Å]	11.256(2)	20.671(4)	13.32(4)	20.7199(4)
c [Å]	21.535(4)	21.063(4)	21.67(6)	21.8066(6)
α [°]	90	90	77.7(2)	90
β [°]	90	90.80(3)	88.3(3)	109.644(3)
γ [°]	90	90	70.7(2)	90
V [Å ³]	5581.0(19)	5107.5(16)	3343(18)	7162.0(3)
Z	2	4	2	4
ρ calc [g·cm ⁻³]	1.465	1.563	1.420	1.610
μ [mm ⁻¹]	2.942	3.173	2.514	4.370
F (000)	2468	2392	1444	3416
θ range [°]	2.01 – 26.00 –28 ≤ <i>h</i> ≤ 27	2.00 – 25.00 –13 ≤ <i>h</i> ≤ 13	1.73 – 24.00 –14 ≤ <i>h</i> ≤ 14	2.20 – 27.00 –21 ≤ <i>h</i> ≤ 21
Index ranges	–13 ≤ <i>k</i> ≤ 13 –26 ≤ <i>l</i> ≤ 26	–24 ≤ <i>k</i> ≤ 22 –25 ≤ <i>l</i> ≤ 25	–14 ≤ <i>k</i> ≤ 15 0 ≤ <i>l</i> ≤ 24	–26 ≤ <i>k</i> ≤ 26 –27 ≤ <i>l</i> ≤ 27
collected reflections	31772	35977	10469	79775
independent reflections	10894 (<i>R</i> _{int} = 0.1009)	8983 (<i>R</i> _{int} = 0.1899)	10469 (<i>R</i> _{int} = 0.0000)	15595 (<i>R</i> _{int} = 0.0510)
Data / Restraints / Parameters	10894 / 1 / 659	8983/0/624	10469 / 1 / 756	15595 / 0 / 841
Goodness-of-fit on F2	1.015	1.023	1.057	1.006
largest diff peak and hole [e Å ⁻³]	3.570 and –1.813	1.324 and –2.229	3.850 and –3.493	2.782 and –1.232
final R indices [<i>I</i> > 2σ(<i>I</i>)]	R1 = 0.0601 wR2 = 0.1591	R1 = 0.0800, wR2 = 0.1979	R1 = 0.0699, wR2 = 0.1791	R1 = 0.0323, wR2 = 0.0670
R indices (all data)	R1 = 0.0674 wR2 = 0.1669	R1 = 0.1168 wR2 = 0.2343	R1 = 0.0811 wR2 = 0.1893	R1 = 0.0584 wR2 = 0.0695

The tendency of strong π -acceptor ligands to occupy in these Fe-Pt systems a bridging position in order to compensate a high electron density by π -back-bonding is also confirmed by treatment of **2b** with SO₂. Theoretical and experimental studies have shown that sulfur dioxide as bridging ligand may exert a π -acceptor propensity exceeding even that of carbon monoxide [22]. This explains why, after short bubbling of SO₂ in a dichloromethane solution of **2b**, the μ -isonitrile ligand is chased away from his bridging position and a μ -SO₂ molecule occupies in [(OC)₂(*o*-anisylNC)Fe(μ -SO₂)(μ -dppa)Pt(PPh₃)] (**4**) its former place with concomitant CO extrusion (Scheme 3).



Scheme 3. Formation of a heterodinuclear μ -SO₂ complex

Both the ³¹P- and ¹⁹⁵Pt NMR data indicate that the metal-metal bonded core skeleton of **4** remained intact (Table 3). From the position of the $\nu(\text{C}\equiv\text{N})$ vibration at 2125 cm⁻¹ it is evident, that the isonitrile is now ligated in a terminal manner. Characteristic for SO₂ in a bridging bonding mode is the presence of an intense symmetric and an asymmetric $\nu(\text{SO})$ -vibration in the range between 1190-1050 cm⁻¹. For example, the occurrence of two vibrations at 1189 and 1049 cm⁻¹ has been reported for [(OC)(Rh(μ -SO₂)(μ -S)(μ -dppm)₂Mn(CO)₂)], and we observed previously two vibrations at 1183 and 1044 cm⁻¹ in the IR spectrum of [(OC)₄W(μ -SO₂)(μ -dppa)Pt(PPh₃)] [23]. Therefore the two strong absorptions observed at 1097 and 1026 cm⁻¹ are attributed to the $\nu(\text{SO})$ stretches of **4**.

2.3. Preparation and reactivity of cationic *N*-alkylated aminocarbyne complexes.

In an analogous manner to the preparation of the μ -aminocarbyne complex [(OC)₃Fe(μ -CN(Me)xylyl)(μ -dppa)Pt(PPh₃)] [BF₄] (**5a**), the cationic derivative [(OC)₃Fe(μ -CN(Me)Bz)(μ -dppa)Pt(PPh₃)] [BF₄] (**5b**) was obtained by electrophilic addition on the basic nitrogen atom of the μ -CNR ligand using the Meerwein salt [Me₃O][BF₄] or methyl triflate as the alkylating agent (Scheme 4). Note that these compounds may alternatively be considered as alkylated iminium salts **A** (Chart 2) [24], but in line with the group of Busetto *et al.* [25], we prefer a description as μ -aminocarbyne complexes **C** (see also the discussion concerning the isomerization of **5h** below) [17, 26, 27] with an important contribution of form **B**.

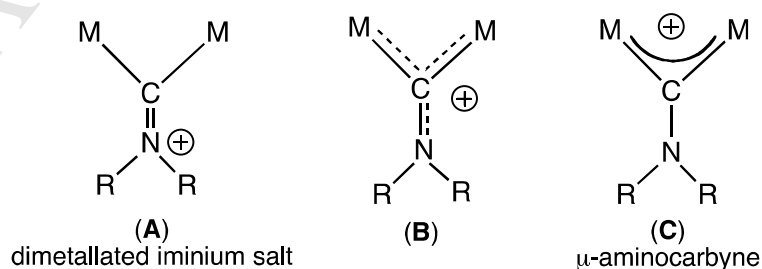
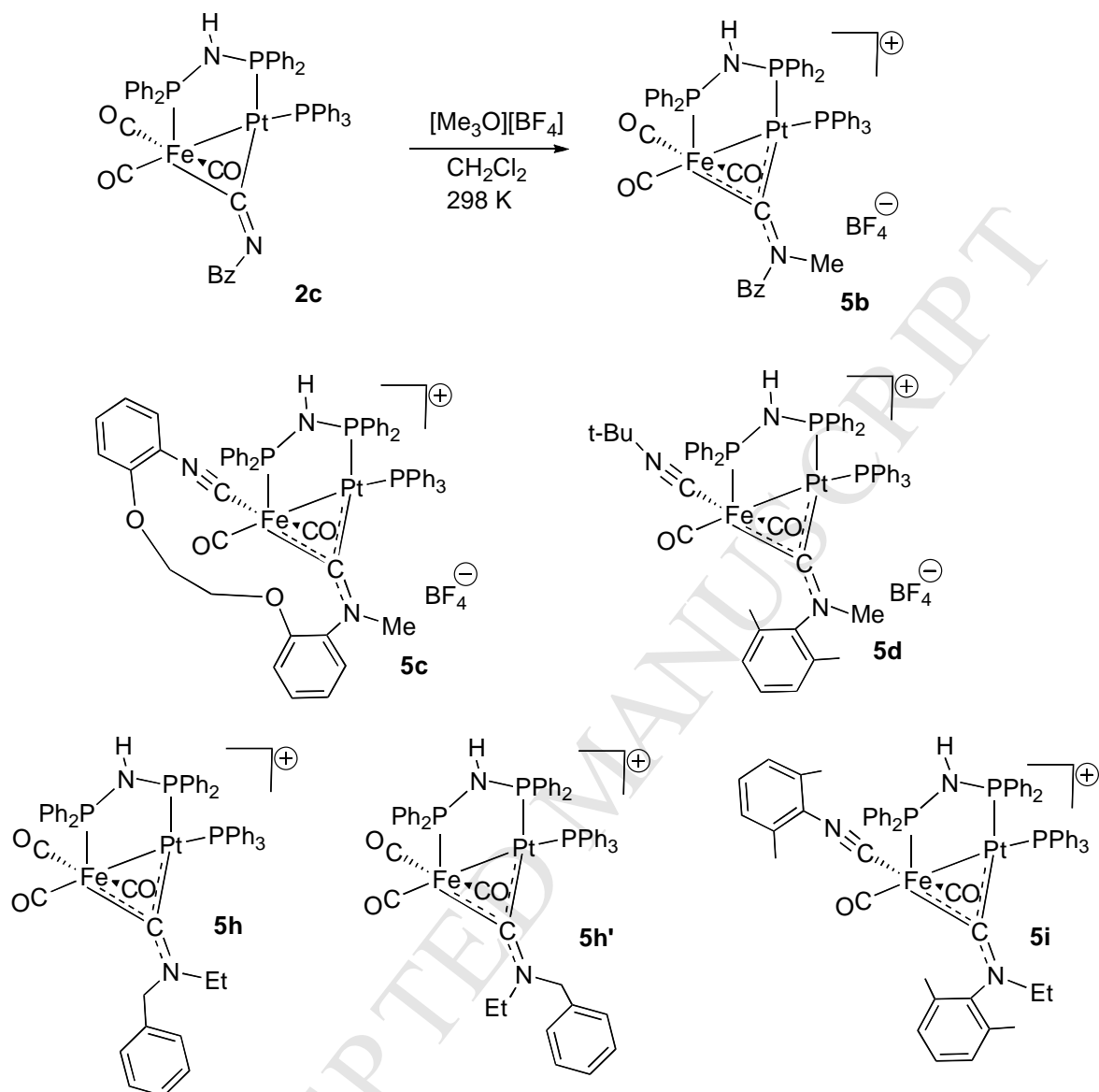


Chart 2

N-methylation allowed also to convert the labile mixed bis(isonitrile) complex **3d** into the stable salt **5d**. Note that the terminal *tert*-BuNC ligand does not react even with an excess of the alkylating agent (Scheme 4).



Scheme 4. Preparation of μ -aminocarbyne complexes **5** by *N*-alkylation.

A priori two isomeric forms are conceivable with the methyl group orientated towards the platinum centre or alternatively towards the $\text{Fe}(\text{CO})_n$ fragment. All ^1H , ^{31}P and ^{195}Pt NMR data indicate the formation of just one isomer (Table 3). To unambiguously ascertain the stereochemistry around the μ_2 -aminocarbyne ligand, X-ray diffraction studies on **5b** and **5d** were undertaken.

Crystal structures of $[(\text{OC})_3\text{Fe}\{\mu\text{-CN}(\text{Me})\text{Bz}\}(\mu\text{-dppa})\text{Pt}(\text{PPh}_3)][\text{BF}_4]$ (**5b**) and $[(\text{OC})_2(\text{tert-BuNC})\text{Fe}\{\mu\text{-CN}(\text{Me})\text{xylyl}\}(\mu\text{-dppa})\text{Pt}(\text{PPh}_3)][\text{BF}_4]$ (**5d**).

Suitable single-crystals of yellow **5b** were grown from $\text{CH}_2\text{Cl}_2/\text{Et}_2\text{O}$. The structure depicted in Figure 3 shows that the μ -aminocarbyne ligand symmetrically bridges [Fe–C(1) 1.905(13), Pt–C(1) 1.989(15) Å] the two metal centers, the separation of which, 2.5182(16) Å, is indicative of the

presence of a metal-metal bond. Due to steric factors, only the isomer with the benzyl group oriented towards the iron center is formed. The short bond length between C(1) and N(1) of 1.330(17) Å reflects the partial C=N double-bond character of the μ -aminocarbyne unit, which, therefore may alternatively be considered as a dimetallated iminium salt ligand (Chart 2). To date, to the best of our knowledge, only one other example of a *heterobimetallic* μ -aminocarbyne complex has been structurally described. A C–N distance of 1.29(2) Å was observed for this tungsten-gold [(CO)₂(Cp)W{ μ -CN(Et)Me}Au(C₆F₅)] complex bridged by a CN(Et)Me ligand [25]. A separation of 2.938 Å between the N atom of the dppa ligand in **5b** and the F(1) atom of the tetrafluoroborate counter ion suggests the presence of a hydrogen-bonding interaction {*d* H(2)⋯F(1) 2.109 Å}. A comparable N⋯F distance of 2.941 Å has been reported for [Ru₂(CO)₄(μ -NO)(μ -H)(μ -P^tBu₂)(μ -dppa)][BF₄] [28], a weaker interaction with the N–H proton [*d*(N⋯F) = 3.105 Å] was found for [(OC)₄Fe(μ -dppa)Pd{CH₂CH₂C(=O)Me}][BF₄] [5c, 29–31].

In the structure of **5d**, which contains both a CH₂Cl₂ and Et₂O molecule of crystallisation, the methyl group of the aminocarbyne ligand points again towards the PtPPh₃ moiety (Figure 4). The C(1)–N(1) bond length of 1.265(12) Å is even shorter than that of **5b**. An intermolecular hydrogen bond between the BF₄[−] counter ion and the N–H group of the dppa ligand is also encountered for this salt {*d*[N(2)⋯F(1)] 2.987 Å; H(2)⋯F(1) 2.163 Å}.

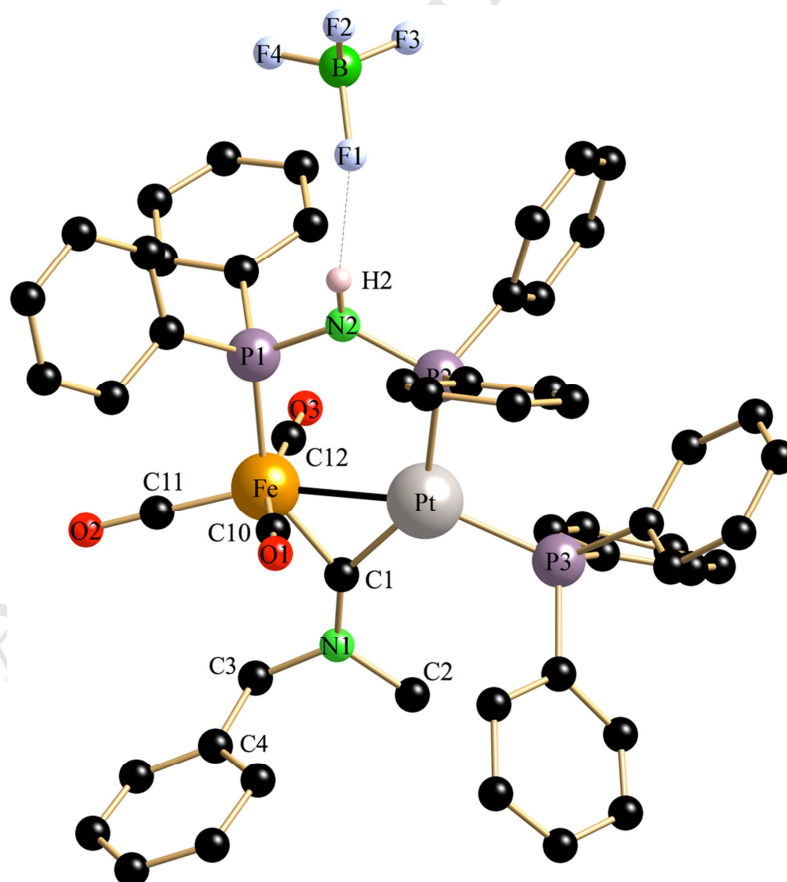


Fig. 3. Perspective view of **5b** showing the atom-labelling scheme. Apart from H(2), all hydrogen atoms have been omitted for clarity. Selected distances (Å) and angles (°): Fe–Pt 2.5182(16), Fe–P(1) 2.232(4), Pt–P(2) 2.328(3), Pt–P(3) 2.293(3), Fe–C(1) 1.905(13), Fe–C(10) 1.775(12), Fe–C(11) 1.775(14), Fe–C(12)

1.822(14), Pt–C(1) 1.989(15), C(1)–N(1) 1.330(17), C(2)–N(1) 1.488(18), N(1)–C(3) 1.452(17), C(10)–O(1) 1.170(14), C(11)–O(2) 1.164(15), C(12)–O(3) 1.136(14), P(1)–N(2) 1.708(9), P(2)–N(2) 1.710(10); P(1)–Fe–Pt 95.95(10), P(2)–Pt–Fe 96.19(8), P(3)–Pt–Fe 156.89(10), P(3)–Pt–P(2) 106.91(11), Pt–C(1)–Fe 80.6(6), C(10)–Fe–Pt 76.1(4), C(11)–Fe–Pt 161.8(5), C(12)–Fe–Pt 88.9(4), C(1)–Pt–P(3) 108.6(4), C(1)–Pt–P(2) 144.4(4), C(1)–Fe–P(1) 146.3(4), N(1)–C(1)–Fe 137.2(10), C(1)–N(1)–C(2) 124.5(12), C(1)–N(1)–C(3) 122.0(12), C(2)–N(1)–C(3) 113.4(13), P(1)–N(2)–P(2) 124.2(6).

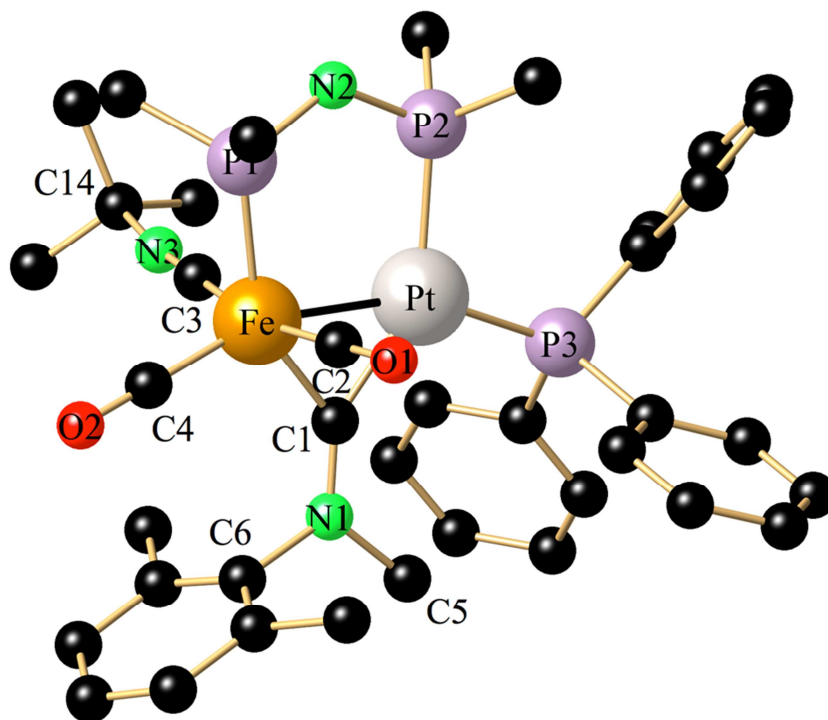


Fig. 4. Perspective view of the cation of **5d** showing the atom-labelling scheme. Hydrogen atoms, the CH_2Cl_2 and Et_2O molecules have been omitted. Only the ipso carbon atoms of the phenyl groups of dppa are shown for clarity. Selected distances (Å) and angles (°): Fe–Pt 2.500(9), Fe–P(1) 2.217(8), Pt–P(2) 2.281(8), Pt–P(3) 2.282(9), Fe–C(1) 1.909(11), Fe–C(2) 1.759(10), Fe–C(3) 1.869(11), Pt–C(1) 1.992(9), C(1)–N(1) 1.265(12), C(5)–N(1) 1.474(13), N(1)–C(6) 1.477(13), C(2)–O(1) 1.145(11), C(4)–O(2) 1.125(11), C(3)–N(3) 1.154(12), P(1)–N(2) 1.678(9), P(2)–N(2) 1.665(10); P(1)–Fe–Pt 96.9(3), P(2)–Pt–Fe 95.3(3), P(3)–Pt–Fe 157.12(13), P(3)–Pt–P(2) 107.5(2), Pt–C(1)–Fe 79.8(4), C(2)–Fe–Pt 84.7(4), C(4)–Fe–Pt 158.1(3), C(3)–Fe–Pt 83.0(4), C(1)–Pt–P(3) 108.6(3), C(1)–Pt–P(2) 143.9(3), C(1)–Fe–P(1) 148.5(3), N(1)–C(1)–Fe 135.9(7), N(3)–C(3)–Fe 178.5(8), C(1)–N(1)–C(5) 124.4(8), C(1)–N(1)–C(6) 122.5(8), C(5)–N(1)–C(6) 113.1(8), C(3)–N(3)–C(14) 174.1(11), P(1)–N(2)–P(2) 126.2(5).

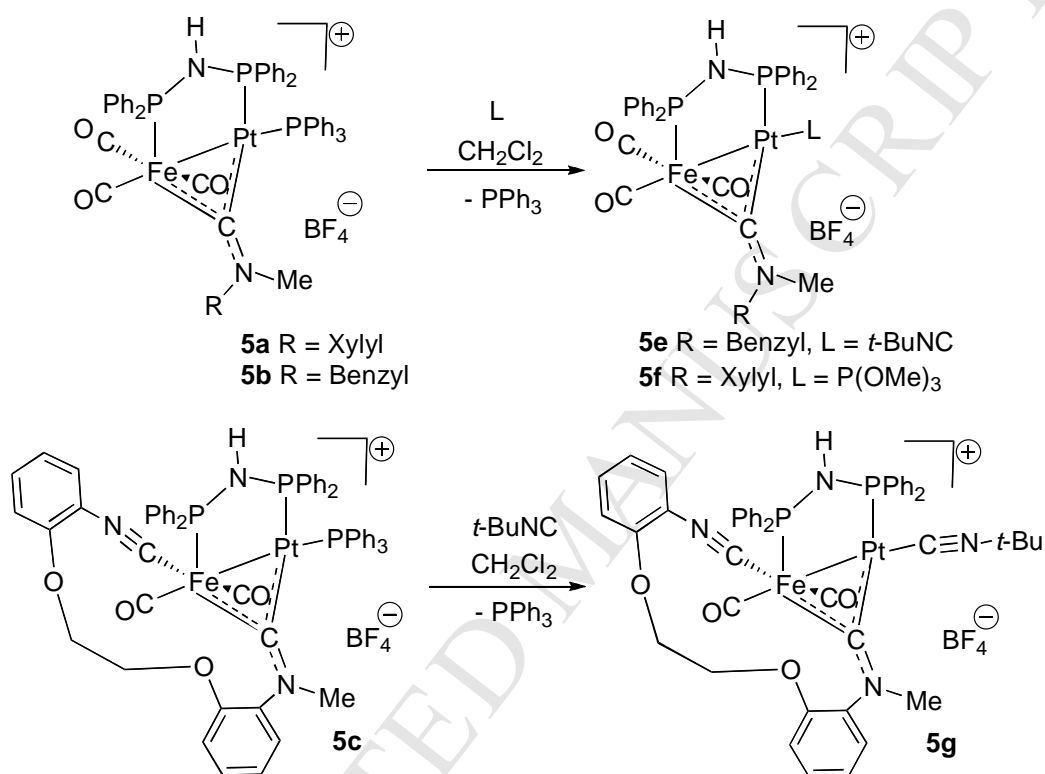
Similarly, *N*-alkylation of **3c** affords the macrocyclic compound **5c**, whose enhanced stability in solution compared to that of precursor **3c** allowed the recording of a ^{13}C NMR spectrum. Characteristic for this type of aminocarbyne complexes is the resonance of the $\mu\text{-C}$ atom, which is observed in the low-field region at $\delta = 315.7$ as a doublet of doublets of doublets with $^2J(\text{P-C})$ coupling constants of 3, 16 and 79 Hz, respectively.

More complicated is the outcome of the *N*-alkylation of **2b** using ethyl triflate leading to $[(OC)_3Fe\{\mu-CN(Et)Bz\}(\mu-dppa)Pt(PPh_3)][OSO_2CF_3]$ (**5h**) (Scheme 4). Initially, the isomer with an orientation of the benzyl group towards the $Fe(CO)_3$ fragment and of the ethyl group toward Pt is formed. NMR monitoring reveals after some hours in solution the appearance of a second set of signals, whose intensity augments steadily. After approximately 24 h the presence of an isomeric mixture of 50% **5h** and 50% **5h'** can be observed. It seems that now a steady state equilibrium is reached, since no further conversion in favor to isomer **5h'** occurs. Recording the ^{31}P NMR at 318 and 228K respectively revealed no shift of the 50:50 ratio between the two isomers. After recrystallization, a crystalline mixture was obtained in which **5h'** is enriched to about 70 %. This finding allows assigning unequivocally the sets of signals in the 1H NMR and ^{31}P NMR spectra to the respective isomer (see Experiment. Section). A restricted rotation around the C-N bond of the trimetallic cluster $[Fe_3(\mu_2-H)(CO)_{10}\{\mu-CN(Et)i-Pr\}]$ has been evidenced by Howell *et al.* via NMR experiments at variable temperature [32]. The isomerization in the case of $5h \rightleftharpoons 5h'$ implies also a restricted rotation around the C-N bond, therefore a description of the complexes of series **5** as μ_2 -aminocarbyne complexes is more appropriate than considering them as dimetallated iminium salts. In contrast, ethylation of **3a** resulted in formation of only one isomeric form of $[(OC)_2(xylyl)NC]Fe\{\mu-CN(Et)xylyl\}(\mu-dppa)Pt(PPh_3)]$ (**5i**), in which the ethyl group is pointing towards the $PtPPh_3$ moiety. The composition of this yellow salt was also ascertained by a FAB^+ mass spectrum exhibiting an intense peak of the cation at m/z 1245, whose experimental isotopic distribution pattern fits with the simulated one.

As discussed above, addition of *tert*-butylisocyanide to **2a** yielded exclusively the carbonyl substitution product **3d**. In contrast, upon addition of an excess of *tert*-BuNC to **5b** no carbonyl substitution takes place. Instead the Pt-bound PPh_3 ligand is replaced by *tert*-BuNC in a regioselective manner to give $[(OC)_3Fe\{\mu-CN(Me)Bz\}(\mu-dppa)Pt(CNBu-t)][BF_4]$ (**5e**) (Scheme 5). ^{31}P NMR monitoring revealed that within 15 min quantitative formation of **5e** occurs as evidenced by the observation of two doublets at $\delta = 125.5$ and $\delta = 45.9$ with a $^{2+3}J(P-P)$ coupling of 152 Hz along with a broad hump at $\delta -1.7$ due to the liberated PPh_3 . In an analogous manner, **5c** reacts quantitatively with *tert*-BuNC to give the mixed isocyanide salt **5g** bearing both a Fe-bound and a Pt-bound terminal CNR ligand. The composition of this yellow salt, whose ^{31}P NMR spectrum is depicted in the SI (Figure S3), was furthermore ascertained by FAB^+ mass spectrometry showing as most intense peak that of cation at m/z 1054. The isotopic distribution of the experimental spectrum matches perfectly with the simulated one.

The nucleophilic trialkylphosphite ligands are known to substitute carbonyl ligands in dinuclear organometallics, [33-35] but there are also some examples of P-C coupling reactions [36-40]. For example, $P(OMe)_3$ reacts with the allenyl ligand in $[Fe_2(CO)_6(\mu-PPh_2)\{\mu-\eta^1:\eta^2-(H)C=C=CH_2\}]$ to

affords the α,β -unsaturated phosphonate-bridged complex $[\text{Fe}_2(\text{CO})_6(\mu\text{-PPh}_2)\{\mu\text{-}\eta^1:\eta^2\text{-}(\text{CH}_3)\text{C}=\text{CH}\{\text{P}=\text{O}(\text{OMe})_2\}\}]$. However, when reacting **5a** with $\text{P}(\text{OMe})_3$, exclusively PPh_3 substitution occurred yielding exclusively $[(\text{OC})_3\text{Fe}\{\mu\text{-CN}(\text{Me})\text{xylyl}\}(\mu\text{-dppa})\text{Pt}\{\text{P}(\text{OMe})_3\}][\text{BF}_4]$ (**5f**). The ^{31}P NMR spectrum (shown in Figure S4) exhibits a doublet of doublets at δ 141.9 with a very strong $^1J(\text{Pt-P})$ coupling of 6088 Hz, characteristic for a Pt-bound $\text{P}(\text{OMe})_3$ ligand. The ^{195}Pt NMR spectrum features the expected ddd pattern at δ -2631 with $J(\text{Pt-P})$ couplings of 6088, 2636 and 69 Hz.



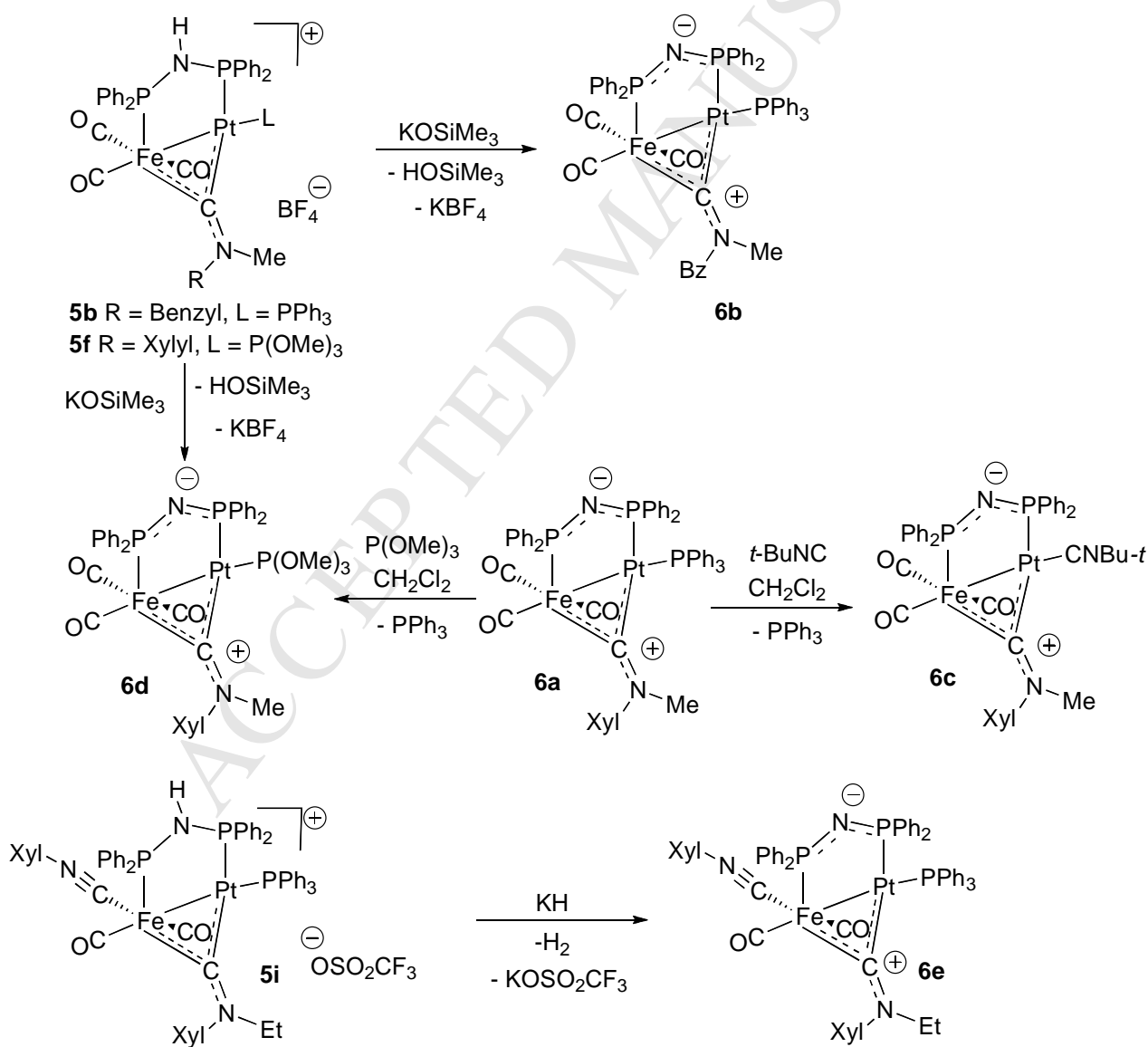
Scheme 5. Site-selective substitution of the Pt-bound PPh_3 ligand by L

2.4. Preparation and reactivity of zwitterionic aminocarbyne complexes

2.4.1 Preparation of zwitterionic aminocarbyne complexes

Due its slightly acidic character, the N-H group of dppa can be easily deprotonated by bases to give bis(diphenylphosphanyl)amide. For example, treatment of dppa with BuLi affords the salt $\text{Li}[\text{Ph}_2\text{PNPPH}_2]$ [41]. The possibility to deprotonate metal-coordinated dppa has been demonstrated for early and late transition metal complexes, selected examples are the mononuclear chelate complexes $[\text{Pd}(\text{Cl})(\text{Ph}_2\text{PNPPH}_2)(\text{PEt}_3)]$ and $[\text{CpFe}(\text{CO})(\text{Ph}_2\text{PNPPH}_2)]$ [42-45]. Ellermann and Braunstein have reported on the deprotonation of homo- and heterodinuclear dppa-spanned complexes [46]. We have communicated several years ago that deprotonation of the dppa-bridge of **5a** occurs even with mild bases such as KOSiMe_3 leading to the structurally characterized zwitterionic aminocarbyne complex $[(\text{OC})_3\text{Fe}\{\mu\text{-CN}(\text{Me})\text{xylyl}\}(\mu\text{-Ph}_2\text{PNPPH}_2)\text{Pt}(\text{PPh}_3)]$ (**6a**) [11]. To explore the scope of the reactivity of these species, we prepared a couple of other

derivatives including examples bearing a terminal CNR ligand. Thus addition of KOSiMe_3 to a CH_2Cl_2 solution of **5b** produces quantitatively the very stable compound $[(\text{OC})_3\text{Fe}\{\mu\text{-CN}(\text{Me})\text{Bz}\}(\mu\text{-Ph}_2\text{PNPPh}_2)\text{Pt}(\text{PPh}_3)]$ (**6b**). Like in **6a**, the resonances in the ^{195}Pt and ^{31}P NMR spectra of **6b** are considerably broadened, whereas the resonance of the Pt-bound PPh_3 ligand gives rise to a well-resolved doublet (See Experimental Section). Addition of an excess of *t*-BuNC to a solution of **6a** did not lead to a carbonyl substitution, ^{31}P NMR monitoring revealed a quantitative replacement of the Pt-bound PPh_3 producing $[(\text{OC})_3\text{Fe}\{\mu\text{-CN}(\text{Me})\text{xyllyl}\}(\mu\text{-Ph}_2\text{PNPPh}_2)\text{Pt}(\text{CNBu-}t)]$ (**6c**) (Scheme 7). Similarly, the PPh_3 ligand is replaced by addition of a slight excess of trimethylphosphite to yield $[(\text{OC})_3\text{Fe}\{\mu\text{-CN}(\text{Me})\text{xyllyl}\}(\mu\text{-Ph}_2\text{PNPPh}_2)\text{Pt}\{\text{P}(\text{OMe})_3\}]$ (**6d**). This yellow microcrystalline zwitterionic complex was alternatively obtained in high yield by deprotonation of $[(\text{OC})_3\text{Fe}\{\mu\text{-CN}(\text{Me})\text{xyllyl}\}(\mu\text{-dppa})\text{Pt}\{\text{P}(\text{OMe})_3\}][\text{BF}_4]$ (**5f**) with KOSiMe_3 .

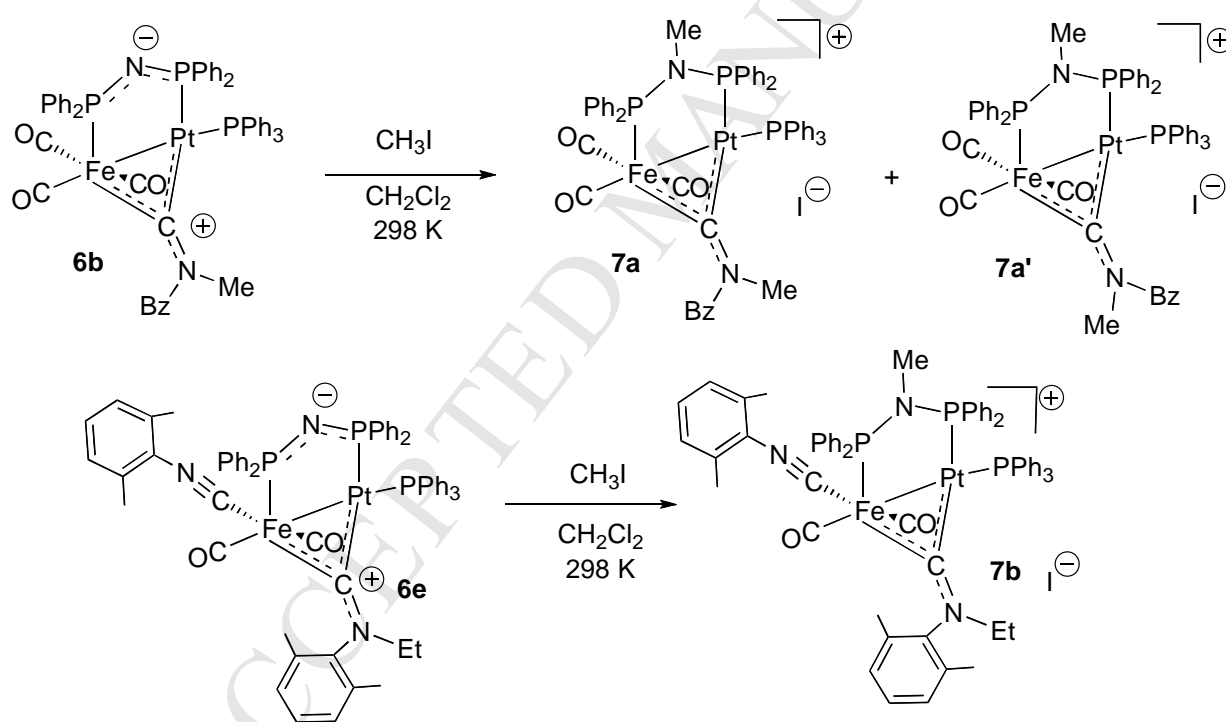


Scheme 6. Preparation of zwitterionic aminocarbene complexes **6**.

The basicity of KOSiMe_3 is not sufficient to deprotonate the more electron-rich isonitrile-substituted complexes $[(\text{OC})_2(\text{xylylNC})\text{Fe}\{\mu\text{-CN}(\text{Et})\text{xylyl}\}(\mu\text{-dppa})\text{Pt}(\text{PPh}_3)]^+$ (**5i**), however the addition of KH to a THF solution allows a fast and quantitative conversion to zwitterionic complex $[(\text{OC})_2(\text{xylylNC})\text{Fe}\{\mu\text{-CN}(\text{Et})\text{xylyl}\}(\mu\text{-Ph}_2\text{PNPPh}_2)\text{Pt}(\text{PPh}_3)]$ (**6e**) (Scheme 6).

2.4.2 Preparation of *N*-alkylated aminocarbene complexes

In the presence of an excess of CH_3I , the amide function of the deprotonated dppa ligand of **6b** is readily methylated forming the yellow salt $[(\text{OC})_3\text{Fe}\{\mu\text{-CN}(\text{Me})\text{Bz}\}\{\mu\text{-Ph}_2\text{PN}(\text{Me})\text{PPh}_2\}\text{Pt}(\text{PPh}_3)][\text{I}]$, which coexists according the NMR data as a 80:20 mixture of isomers **7a** and **7a'** (Scheme 7 and Figure S5). We assume that this coexistence of two isomeric forms is again due to a restricted rotation around the C-N bond, as already discussed in the case of the **5h** \rightleftharpoons **5h'** interconversion.



Scheme 7. *N*-methylation of the zwitterionic aminocarbene complexes **6**.

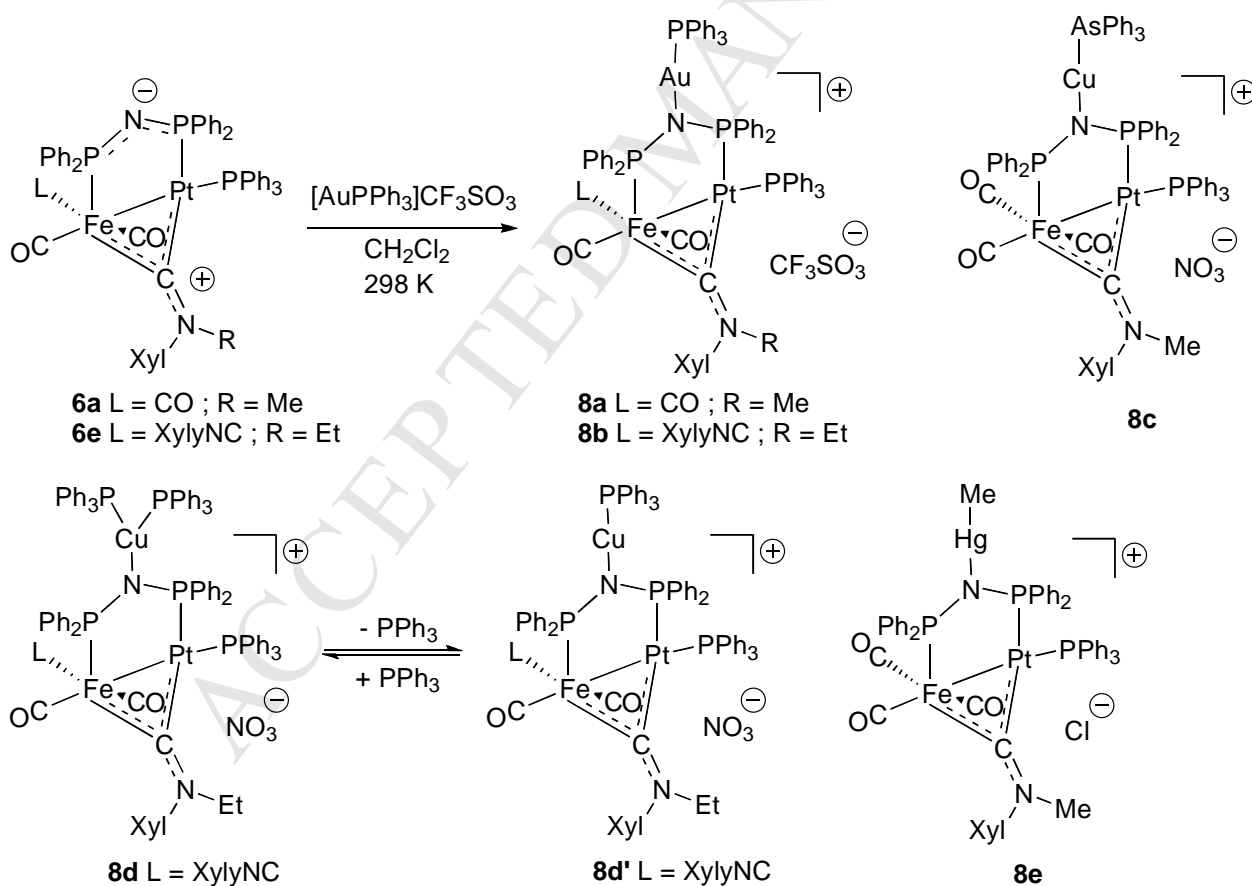
Quantitative *N*-methylation of the P-N-P backbone also occurs after agitation of a solution of the zwitterionic complex **6e** in the presence of an excess of CH_3I to produce $[(\text{OC})_2(\text{xylylNC})\text{Fe}\{\mu\text{-CN}(\text{Et})\text{xylyl}\}\{\mu\text{-Ph}_2\text{PN}(\text{Me})\text{PPh}_2\}\text{Pt}(\text{PPh}_3)][\text{I}]$ (**7b**). The formation of a bis(diphenylphosphino)methylamine-bridge was evidenced from the ^1H NMR spectrum, which displays a triplet ($^3J(\text{P-H}) = 6.1$ Hz) at δ 2.45 due to the N-Me group. Compared to the dppa-bridged derivative $[(\text{OC})_2(\text{xylylNC})\text{Fe}\{\mu\text{-CN}(\text{Et})\text{xylyl}\}(\mu\text{-dppa})\text{Pt}(\text{PPh}_3)][\text{OSO}_2\text{CF}_3]$ **5i**, the *N*-

methylation causes a significant low-field shift of the diphosphine resonances to δ 124.0 and 99.2 ppm, whereas the signal of the PPh_3 ligand at δ 33.0 has the same chemical shift as in **5i**.

ACCEPTED MANUSCRIPT

2.4.3 Preparation of heterotrimetallic aminocarbene complexes

Ellermann has reported that reaction of $\text{Li}[\text{Ph}_2\text{PNPPh}_2]$ with PPh_3AuCl does not lead to the gold amide complex $[\text{Ph}_2\text{PN}(\text{AuPPh}_3)\text{PPh}_2]$, but to formation of the dinuclear species $[\text{Au}(\text{Ph}_2\text{P})_2\text{N}]_2$ with dissociation of triphenylphosphine [47a]. In contrast, the lithiated chelate complexes $\text{Li}[(\text{OC})_4\text{M}(\text{Ph}_2\text{PNPPh}_2)]$ ($\text{M} = \text{Cr}, \text{Mo}, \text{W}$) have been converted to the heterodinuclear compounds $[(\text{OC})_4\text{M}\{\text{Ph}_2\text{PN}(\text{AuPPh}_3)\text{PPh}_2\}]$ [47b]. This intrigued us whether the zwitterionic compounds of type **6** could be used to construct heterotrimetallic complexes by reaction with electrophilic coinage metal salts. Initial attempts to react **6a** with PPh_3AuCl were not straightforward, but using *in situ* generated $[\text{AuPPh}_3][\text{OSO}_2\text{CF}_3]$ allowed the isolation of the heterotrimeric gold-amide complex $[(\text{OC})_3\text{Fe}\{\mu\text{-CN}(\text{Me})\text{xyllyl}\}\{\mu\text{-Ph}_2\text{PN}(\text{AuPPh}_3)\text{PPh}_2\}\text{Pt}(\text{PPh}_3)][\text{OSO}_2\text{CF}_3]$ (**8a**) in 58% yield in form of air-stable bright-yellow crystals (Scheme 8).



Scheme 8. Preparation of heterotrimetallic aminocarbene complexes **8**.

The structure of the trimetallic core of **8a** can be deduced from the combination of ^{31}P - and ^{195}Pt -NMR spectra. As encountered in the bimetallic μ -aminocarbene complexes presented above,

the $^{31}\text{P}\{^1\text{H}\}$ -NMR spectrum consists of three mutually coupled signals at δ 105.6, 87.0 and 34.8, which are assigned to the iron- and platinum-bound dppa nuclei as well as to the Pt-bound PPh_3 ligand. The resulting doublet of doublets pattern is splitted again by coupling with the PPh_3 ligand coordinated on the gold atom ($\delta = 32.3$), so finally the signals appear in form of a doublet of doublets of doublets. Furthermore, each ddd resonance is flanked by ^{195}Pt satellites. These Pt-P couplings are detailed in the $^{195}\text{Pt}\{^1\text{H}\}$ NMR spectrum depicted in Figure 5. Note that due to an accidentally identical magnitude of the $^{2+3}J(\text{Pt-P})$ and $^4J(\text{Pt-P})$ coupling of around 66 Hz, the pattern of the signal centered at $\delta = -2618$ appears as a doublet of doublets of triplets.

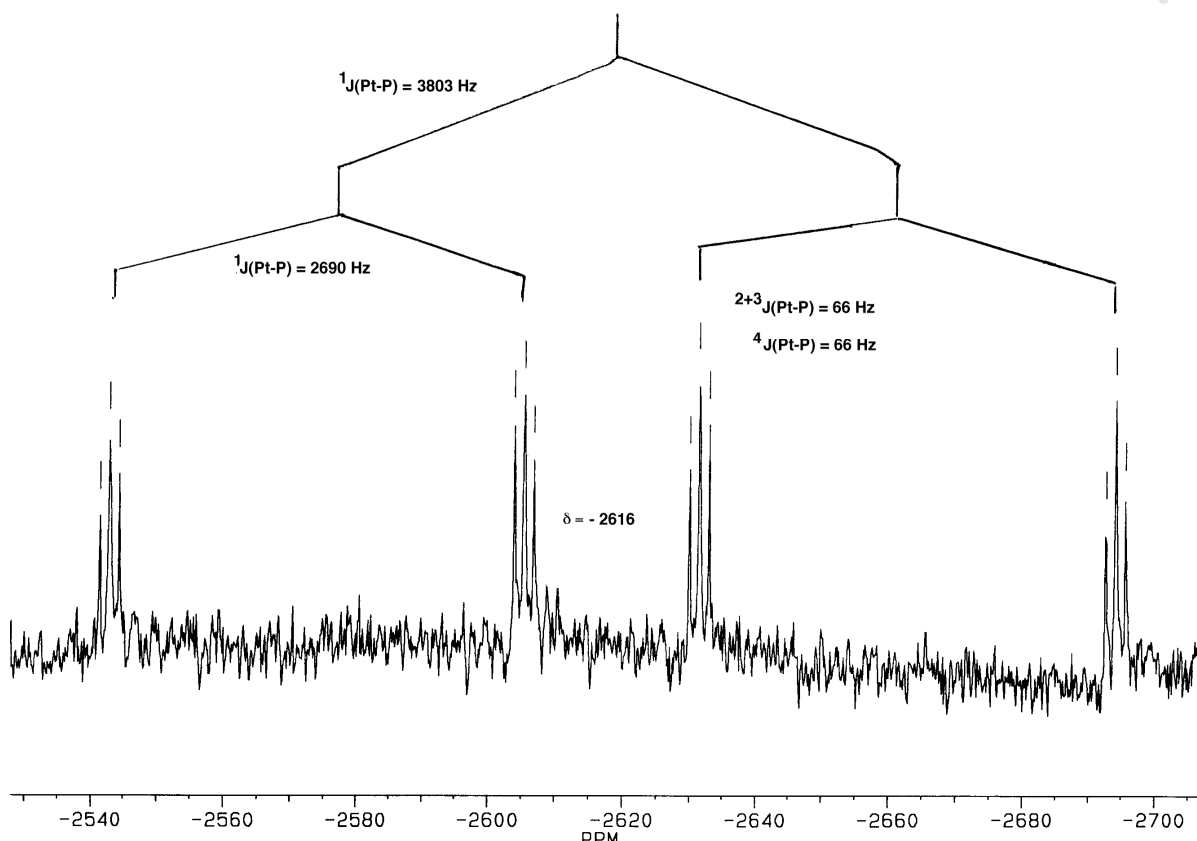


Fig. 5. $^{195}\text{Pt}\{^1\text{H}\}$ NMR spectrum of heterotrimetallic complex **8a** in CDCl_3 at 298 K

*Crystal structure of $[(\text{OC})_3\text{Fe}\{\mu\text{-CN}(\text{Me})\text{xylyl}\}\{\mu\text{-Ph}_2\text{PN}(\text{AuPPh}_3)\text{PPh}_2\}\text{Pt}(\text{PPh}_3)][\text{OSO}_2\text{CF}_3]$ (**8a**).* Suitable single-crystals of **8a** were grown from $\text{CH}_2\text{Cl}_2/\text{Et}_2\text{O}$. The structure of this salt crystallizing in the monoclinic space group $\text{P}2_1/\text{n}$ is shown in Figure 6. The Fe–Pt bond distance of 2.4932(6) Å is very similar with that of **5d**. Like in precursor **6a**, the xylyl group of the aminocarbonyl ligand points towards the sterically less crowded $\text{Fe}(\text{CO})_3$ fragment. The N–P–Au array of the gold-amid fragment is almost linear [$\text{N}(1)\text{-Au-P}(1) = 174.26(10)^\circ$]. The bond length of the covalent Au–N(1) amide bond amounts to 2.053(4) Å and may be compared with that of the trinuclear complex $[\text{C}_6\text{H}_4\{\text{NHPPH}_2\text{Au}(\text{C}_6\text{F}_5)_3\}\{\text{N}(\text{AuPPh}_3)\text{PPh}_2\text{Au}(\text{C}_6\text{F}_5)_3\}]$ 2.096(4) [48]. Also the Au–P(1) distances are quite comparable in both compounds [2.2213(13) vs. 2.2404(16) Å].

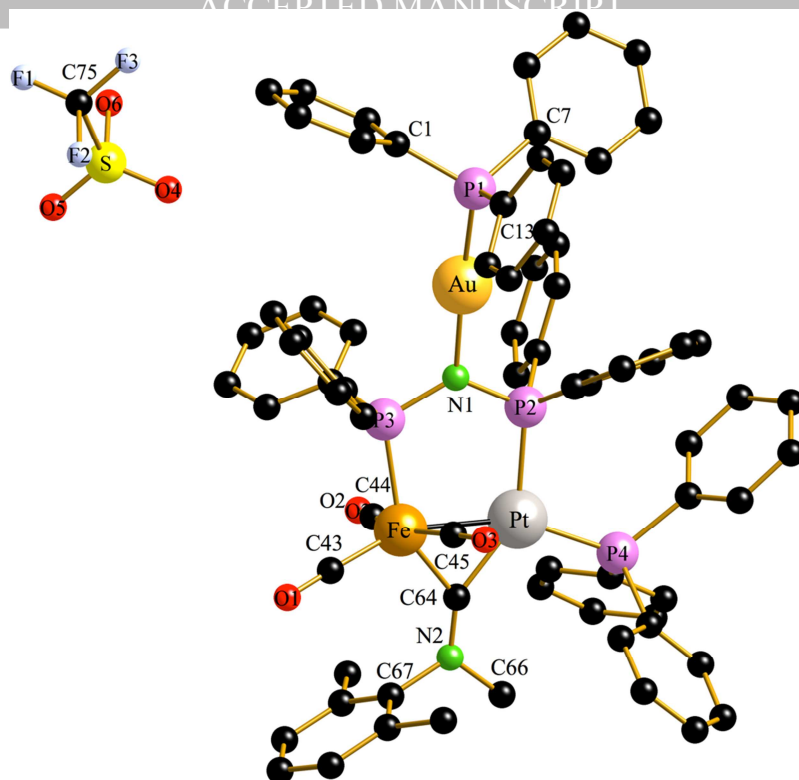


Fig. 6. Perspective view of **8a** showing the atom-labelling scheme. Hydrogen atoms have been omitted for clarity. Selected distances (Å) and angles (°): Fe–Pt 2.4932(6), Fe–P(3) 2.2576(13), Pt–P(2) 2.2930(12), Pt–P(4) 2.2730(11), Fe–C(43) 1.781(5), Fe–C(44) 1.787(5), Fe–C(45) 1.793(5), Fe–C(64) 1.929(4), Pt–C(64) 1.987(4), C(64)–N(2) 1.276(5), C(67)–N(2) 1.456(5), N(2)–C(66) 1.475(5), C(43)–O(1) 1.144(5), C(44)–O(2) 1.143(5), C(45)–O(3) 1.139(5), P(2)–N(1) 1.681(4), P(3)–N(1) 1.664(3), Au–N(1) 2.053(4), Au–P(1) 2.2212(13); P(3)–Fe–Pt 96.03(4), P(2)–Pt–Fe 94.56(3), P(4)–Pt–Fe 157.25(3), P(4)–Pt–P(2) 108.05(4), Pt–C(64)–Fe 79.09(16), C(43)–Fe–Pt 156.70(15), C(44)–Fe–Pt 87.49(14), C(45)–Fe–Pt 74.48(14), C(64)–Pt–P(4) 107.97(13), C(64)–Pt–P(2) 143.97(12), C(64)–Fe–P(3) 146.55(13), N(2)–C(64)–Fe 136.8(3), C(64)–N(2)–C(67) 121.8(4), C(64)–N(2)–C(66) 124.0(4), P(3)–N(1)–P(2) 122.1(2), Au–N(1)–P(2) 116.61(18), Au–N(1)–P(3) 121.23(19), N(1)–Au–P(1) 174.26(10).

In a similar manner, the yellow heterotrimeric salt $[(OC)_2(xylyl)NC]Fe\{\mu-CN(Et)xylyl\}\{\mu-Ph_2PN(AuPPh_3)PPh_2\}Pt(PPh_3)][OSO_2CF_3]$ (**8b**) was obtained by reaction of **6e** with $[AuPPh_3][OSO_2CF_3]$ (Scheme 8). This yellow compound was characterized by IR spectroscopy and multinuclear NMR techniques (Table 3). Noteworthy is the ^{195}Pt NMR spectra shown in Figure S6 in the SI. In contrast to the spectrum of **8a**, now 4 distinct Pt–P couplings are present. Therefore the resonance centered at δ -2672 is splitted into a doublet of doublets of doublets of doublets pattern, with $^{2+3}J(P^1-Pt) = 60$, $^4J(P^4-Pt) = 81$, $^1J(P^2-Pt) = 2774$ and $^1J(P^3-Pt) = 3577$ Hz. All solution data match perfectly with those of an X-ray diffraction study.

Crystal structure of $[(OC)_2(xylyl)NC)Fe\{\mu-CN(Et)xylyl\}\{\mu-Ph_2PN(AuPPh_3)PPh_2\}Pt(PPh_3)] [OSO_2CF_3]$ **8b**

Suitable crystals of **8b**·CH₂Cl₂ were obtained from CH₂Cl₂/Et₂O. The structure of this compound is presented in Fig. S7 in the Supporting Information, together with selected bond length and angles. Since the overall structures of **8b** is very reminiscent to that of **8a**, only the most relevant features are discussed. The Fe–Pt bond distance of **8b** is almost identical to that of **8a** (2.4943(13) vs. 2.4932(6) Å). The linear terminal iron-bound isonitrile ligand is orthogonal with respect to the metal–metal bond, the angle Fe–Pt–C(14) being 93.5(3)°. Within the gold-amide fragment, the N–P–Au array is almost linear [N(2)–Au–P(4) = 176.2(2)°]. The bond length of the covalent Au–N(2) bond amounts to 2.060(6) Å, the Au–P(4) distance 2.215(2) Å. The P(1)–N(2) and P(2)–N(2) distances of 1.655(7) and 1.672(6) Å also match with those of **8a**.

Spectroscopic properties of 8a.

Many articles concerning the photophysical behaviour of platinum complexes bearing phosphine ligands are reported in the literature [49]. There are also several reports on the luminescence properties of gold complexes [50]; for example the Au(I)PR₃ fragment is known to exhibit luminescence both in the solid state and in solution [51]. It was therefore of interest to investigate the trinuclear complex **8a** containing these two heavy metals. The normalized electronic absorption and emission spectra recorded in CH₂Cl₂ and in the solid state are shown in Figure 7. Absorption and emission spectral data obtained in solution and in the solid state are summarized in Table 2. The absorption spectrum of **8a** is dominated by the phosphine and MeXylyl π,π^* transitions at 247 and 278 nm. After excitation at 370 nm, **8a** exhibits the emission maximum at 434 nm. This emission band was also observed for the dinuclear complex **5a** (Table 2, Fig. S8), thus confirming that there is no significant contribution of the AuPPh₃ fragments. The emission intensity of **8a** in 2-MeTHF (Fig. S9) increases when the temperature decreases and leads to the conclusion that it is phosphorescence centered on the phosphine ligand as assigned for [Au(PPh₃)₂][PF₆] [50a] or [Cu(PPh₃)₂][BH₄] [52]. After excitation at 380 nm, the emission spectra recorded in the solid state for complexes **5a** (Fig. S8) and **8a** (Fig. 7) are similar and show two bands, a high energy (HE) band around 438 nm and a low energy (LE) band about 668 nm. The HE band in the spectra of **5a** and **8a** observed in solution is assigned to the emission centered on the phosphine ligands. The LE band is due either to emission from a platinum-based state or to an excimer present in the solid state. The large Stokes shift of this emission is typical of metal-based states in similar compounds [53].

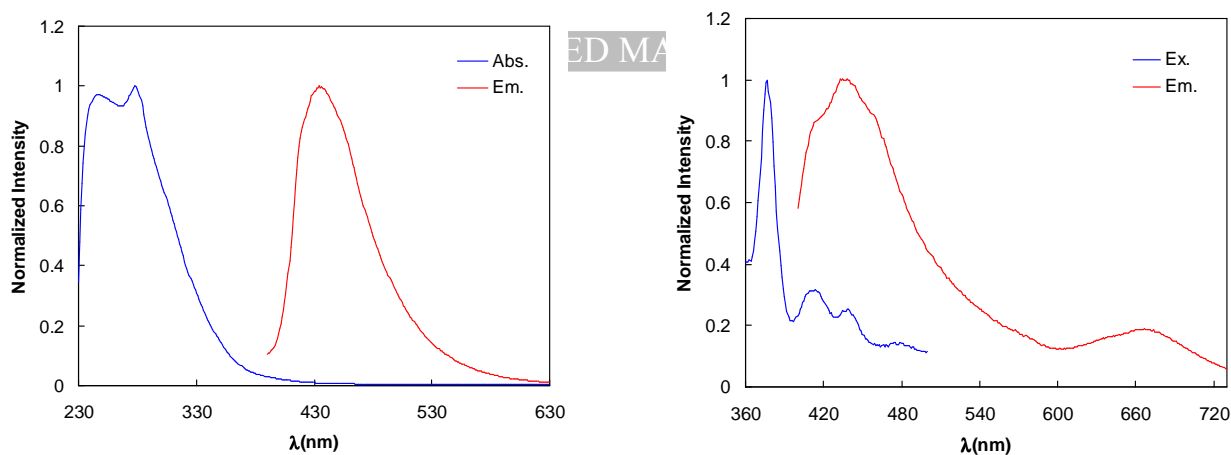


Fig. 7. Normalized absorption (blue) and emission (red) spectra of **8a** recorded in CH_2Cl_2 at 298K (left) and in the solid state at 298K (right).

Table 2. Absorption and emission spectral data obtained for **5a** and **8a**.

Complex	Absorption		Emission	
	CH_2Cl_2 at 298 K $\lambda_{\text{abs}}/\text{nm}$ ($\epsilon/\text{L mol}^{-1} \text{cm}^{-1}$)	CH_2Cl_2 at 298 K $\lambda_{\text{em}}/\text{nm}[\lambda_{\text{excit}}/\text{nm}]$	solid at 298 K $\lambda_{\text{em}}/\text{nm} [\lambda_{\text{excit}}/\text{nm}]$	2-MeTHF $\lambda_{\text{em}}/\text{nm} [\lambda_{\text{excit}}/\text{nm}]$
5a	232 (24150), 277 (sh) (5000)	433[370]	439, 670 [380]	-
8a	247 (22760), 278 (23450)	434[370]	436, 667 [380]	415[370]

The related trimetallic aminocarbyne complex $[(\text{OC})_2(\text{xylylNC})\text{Fe}\{\mu\text{-CN}(\text{Et})\text{xylyl}\}\{\mu\text{-Ph}_2\text{PN}(\text{CuPPh}_3)\text{PPh}_2\}\text{Pt}(\text{PPh}_3)][\text{NO}_3]$ (**8d**) bearing a Cu-N bond was obtained by treatment of **6e** with $[\text{Cu}(\text{PPh}_3)_2][\text{NO}_3]$ [54a]. Unfortunately, due to its lability in solution no satisfying elemental analysis could be obtained. Thus our tentative structural proposition for **8d** is essentially based on the $^{31}\text{P}\{^1\text{H}\}$ NMR spectrum recorded at 233 K. This shows two signals at δ 105.1 (dd, $^{2+3}J(\text{P-P}) = 129$ Hz, $^{3+4}J(\text{P-P}) = 12$ Hz), 83.6 (dd, $^2J(\text{P-P}) = 12$ Hz) for the phosphorous nuclei of the diphosphine and a triplet at 34.6 for the Pt-bound PPh_3 ligand. Two further very broadened signals at δ 9.9 and -0.4 are attributed to the two Cu-bound PPh_3 ligands. This broadening could be on the one hand due to the quadrupole moment of the Cu-isotopes ^{63}Cu (69% natural abundance) and ^{65}Cu (31% natural abundance) with $I = 3/2$. However, upon raising the temperature a progressive broadening, notably that of the high-field signal was noticed, which gets shifted towards the resonance for uncoordinated PPh_3 ($\delta = -4.5$). At ambient temperature, the three low-field signals of the Fe-Pt core remain well resolved; in contrast the resonances at δ 10.0 and -2.0 are collapsed to broad "humps". We therefore suggest a partial dissociation of one of the Cu-bound PPh_3 occurs, which is slowed down at low temperature. The interpretation of the NMR data is hampered by the lability of the Cu-N amide bond. During several attempts to grow single-crystals, the aminocarbyne complex $[(\text{OC})_2(\text{xylylNC})\text{Fe}\{\mu\text{-CN}(\text{Et})\text{xylyl}\}(\mu\text{-dppa})\text{Pt}(\text{PPh}_3)][\text{NO}_3]\cdot\text{O}=\text{PPh}_3$ (**5i'**) has been isolated, in which a $\text{O}=\text{PPh}_3$ ligand is attached through a hydrogen bridge on the dppa ligand [55, 56]. The coordination of triphenylphosphine oxide via a $\text{N-H}\cdots\text{O}$ -bridge is obvious from the IR-

and ^{31}P NMR spectra. A broad N-H absorption at 3130 cm^{-1} , as well as overtone/combination vibration at 2667 cm^{-1} are characteristic for the presence of a hydrogen bridge.

We reacted also **6a** with $[\text{Cu}(\text{AsPh}_3)_3][\text{NO}_3]$ [**54b**] and succeeded to isolate $[(\text{OC})_3\text{Fe}\{\mu\text{-CN}(\text{Me})\text{xylyl}\}\{\mu\text{-Ph}_2\text{PN}(\text{CuAsPh}_3)\text{PPh}_2\}\text{Pt}(\text{PPh}_3)][\text{OSO}_2\text{CF}_3]$ (**8c**) in 51% yield (Scheme 8). Whereas the resonances in the ^{31}P NMR spectrum are well-resolved, the ^{195}Pt NMR spectrum exhibits a very broadened doublet of doublet centered at δ -2584. According the elemental analysis obtained for this microcrystalline bright-yellow product, only one AsPh_3 ligand is ligated on the copper atom. **8c** is moderately stable in the solid state, but NMR monitoring reveals that in solution like in the case of **8d** progressively rupture of the Cu-N amide bond occurs giving $[(\text{OC})_3\text{Fe}\{\mu\text{-CN}(\text{Me})\text{xylyl}\}(\mu\text{-dppa})\text{Pt}(\text{PPh}_3)][\text{NO}_3]$ (**5a'**). The cleavage product **5a'** was also the sole product which could be isolated when attempting to react **6a** with $[\text{Ag}(\text{AsPh}_3)_3][\text{NO}_3]$ [**57**].

We also failed to obtain any metallation product when reacting **6a** with Me_3SnCl and Me_3PbCl , only quantitative formation of $[(\text{OC})_3\text{Fe}\{\mu\text{-CN}(\text{Me})\text{xylyl}\}(\mu\text{-dppa})\text{Pt}(\text{PPh}_3)][\text{Cl}]$ was noticed [**58**]. However, treatment of **6a** and **6e** with MeHgCl afforded the mercurated heterotrimeric amide complexes $[(\text{OC})_2(\text{L})\text{Fe}\{\mu\text{-CN}(\text{R})\text{xylyl}\}\{\mu\text{-Ph}_2\text{PN}(\text{HgMe})\text{PPh}_2\}\text{Pt}(\text{PPh}_3)][\text{Cl}]$ **8e** ($\text{L} = \text{CO}$; $\text{R} = \text{Me}$) and **8f** ($\text{L} = \text{xylylNC}$; $\text{R} = \text{Et}$). Characteristic for these yellowish solids is the observation of a singlet resonance in the ^1H NMR spectra, whose $^2J(^{199}\text{Hg}\text{-H})$ couplings of 202.0 and 204.5 Hz are in the range reported for other methylmercury(II) amides [**59**].

3. Conclusion and Perspectives

We have demonstrated that the bonding mode (bridging vs. terminal) of the CNR ligand in these dppa-spanned Fe-Pt complexes is governed by the electronic propensity of the isonitrile. A strongly donating CNR ligand such as CNBu^t occupies a terminal site on Fe, whereas isonitriles with a more pronounced π -acceptor character prefer a bridging position. Also the coordination of a second CNR ligand is electronically controlled (site-selectivity). Whereas in the case of $[(\text{OC})_3\text{Fe}(\mu\text{-CN-R})(\mu\text{-dppa})\text{Pt}(\text{PPh}_3)]$ (**2**) a Fe-bound carbonyl is substituted to give $[(\text{OC})_2(\text{RNC})\text{Fe}(\mu\text{-CN-R})(\mu\text{-dppa})\text{Pt}(\text{PPh}_3)]$ (**3**), the addition of CNR to the aminocarbyne complexes $[(\text{OC})_3\text{Fe}\{\mu\text{-CN}(\text{R})\text{R}'\}(\mu\text{-dppa})\text{Pt}(\text{PPh}_3)]^+$ leads exclusively to substitution of the Pt-bound PPh_3 ligand. The cationic aminocarbyne salts $[(\text{OC})_2(\text{L})\text{Fe}\{\mu\text{-CN}(\text{R})\text{R}'\}(\mu\text{-dppa})\text{Pt}(\text{PPh}_3)]^+$ (**5** $\text{R}' = \text{Me}, \text{Et}$), which are conveniently prepared by *N*-alkylation using $[\text{Me}_3\text{O}][\text{BF}_4]$ or ethyl triflate, are readily deprotonated by bases to yield the zwitterionic aminocarbynes $[(\text{OC})_2(\text{L})\text{Fe}\{\mu\text{-CN}(\text{R})\text{R}'\}(\mu\text{-Ph}_2\text{PNPPH}_2)\text{Pt}(\text{PPh}_3)]$ (**6**). These latter in turn can be converted to heterotrimetallic species by *N*-metallation using $[\text{AuPPh}_3]^+$, $[\text{CuPPh}_3]^+$, $[\text{CuAsPh}_3]^+$ and ClHgMe as electrophiles. We are currently investigating the reactivity of these μ -aminocarbyne complexes towards unsaturated molecules such as alkenes and alkynes for C-C coupling reactions [**60**].

Table 3. Selected $^{31}\text{P}\{^1\text{H}\}$ - and $^{195}\text{Pt}\{^1\text{H}\}$ NMR data (δ in ppm and J in Hz) at 298K, in CDCl_3

Complex	$\delta(\text{P}^1)$	$\delta(\text{P}^2)$	$\delta(\text{P}^3)$	$^{2+3}J(\text{P}^1-\text{P}^2)$; $^2J(\text{P}^2-\text{P}^3)$; $^3J(\text{P}^1-\text{P}^3)$; $^1J(\text{Pt}-\text{P}^2)$; $^1J(\text{Pt}-\text{P}^3)$; $^{2+3}J(\text{Pt}-\text{P}^1)$	$\delta(^{195}\text{Pt})$
2c	113.8 dd	88.7 dd	38.8 dd	175; 45; 9; 2897; 4275; 42	-2690 ddd
2d	112.8 dd	88.2 dd	37.8 dd	170; 40; 10; 2862; 4267; 41	-2969 ddd
2e	112.1 dd	87.8 dd	37.2 dd	164; 40; 10; 2830; 4248; 47	-2680 ddd
2f	114.4 dd	89.0 dd	37.7 dd	180; 45; 8; 2891; 4297; 48	–
2f'	118.0 d	92.8 dd	42.1 d	213; 62; ND; ND; ND; ND	–
2g	117.9 d	93.3 dd	41.7 d	212; 62; ND; 2868; 4628; ND	-2544 ddd
3b	113.3 dd	88.5 dd	38.3 dd	184; 58; 10; 2956; 4172; ND	–
3c	113.9 dd	88.8 dd	39.1 dd	185; 54; 10; 2950; 4188; ND	–
3d	112.8 dd	89.8 dd	41.3 dd	195; 59; 8; 2973; 4132; ND	–
4	114.4 dd	80.3 dd	30.0 dd	158; 32; 10; 3375; 4050; 45	-3102 ddd
5b	102.7 dd	80.6 dd	34.6 dd	100; 9; 13; 2808; 3793; 72	-2715 ddd
5c	104.6 dd	81.3 dd	33.7 dd	110; 18; 14; 2963; 3656; 76	-2809 ddd
5d	103.1 dd	82.2 dd	34.3 dd	114; 19; 13; 2981; 3603; 69	-2836 ddd
5e	125.5 d	45.9 d		152; 3920; ND	–
5f	102.7 dd	79.8 dd	141.9, dd	106; 10; 19 2636; 6088; 69	-2631 ddd
5g	108.1 d	77.1 d		119; 2876; 82	-2587 dd br
5h	102.1 dd	80.2 dd	34.6 dd	100; 7; 13; 2819; 3802; 71	–
5h'	101.7 dd	79.8 dd	33.5 dd	100; 7; 13; 2811; 3781; 71	–
5i	103.8 dd	81.5 dd	33.2 tr	109; 17; 2924; 3590; 72	-2791 ddd
6b	86.6 dd br	72.0 d	35.9 d	129; 14; ND; 2521; 3748	-2470 dd br
6c	103.7 d br	77.0 d br		112; ND, 2730	–
6d	87.9 dd	70.4 dd	145.9 dd	131; 11; 18; 2374; 6019; 61	-2440 dd
6e	85.4 br	70.7 d br	34.9 dd	136; 15; 9; ND; 3452; ND	–
7a	121.8 dd	97.8 dd	34.2 t	121; 12; 12; 2876; 3858; ND	-2758 ddd
7a'	121.8 dd	97.5 dd	32.9 t	121; 11; 12; 2876; 3821; ND	-2789 ddd
7b	124.0 dd	99.2 dd	33.0 dd	130; 19; 13; 2985; 3694; 72	-2834 ddd
8a^b	105.6 ddd	87.0 ddd	34.8 ddd	115; 7; 13; 2689; 3808; 64	-2618 ddt
8b^c	106.4 ddd	87.7 ddd	33.8 dt	125; 13; 15; 2774; 3577; 60	-2672 dddd
8c	101.9 dd	83.7 dd	35.6 dd	121; 5; 12; 2819; 3819; 69	-2584 dd, br
8d^d	105.1 dd	83.6 dd	34.6 t	129; 12; 12; 2754; 3568; ND	
8e^e	102.5 dd	80.7 dd	34.3 t	102; 11; 9; 2834; 3813; 70	–
8f	109.0 d br	84.9 d br	33.7 t	102; 14; ND; 3584; ND; ND	–

$\text{P}^1 = \text{P}_{\text{Fe}}$; $\text{P}^2 = \text{P}_{\text{Pt}}$; $\text{P}^3 = \text{PR}_3$. ND = Not determined. ^a δ at 243 K. ^b δ ($\text{PPh}_{3\text{Au}}$) = 32.3, “q”, $J(\text{P}-\text{P}) = 5$ Hz, $^4J(\text{Pt}-\text{PPh}_{3\text{Au}}) = 68$ Hz. ^c δ ($\text{PPh}_{3\text{Au}}$) = 32.5, “q”, $J(\text{P}-\text{P}) = 5$ Hz, $^4J(\text{Pt}-\text{PPh}_{3\text{Au}}) = 81$ Hz. ^d δ ($\text{PPh}_{3\text{Cu}}$) = 9.9, s; -0.4, s, br. ^e δ at 253 K.

4. Experimental

All reactions were performed in Schlenk-tube flasks under purified nitrogen. Solvents were dried and distilled under nitrogen before use, toluene and hexane over sodium, dichloromethane from P₄O₁₀. – IR spectra have been recorded on a Nicolet Nexus 470 spectrometer. - Elemental C, H, N analyses were performed on a Leco Elemental Analyser CHN 900. - The ¹H and ³¹P{¹H} NMR spectra were recorded at 313.13 and 121.50 MHz₂ respectively, on a Bruker Avance 300 instrument, or on a Bruker ACP 200 machine (200.13 and 81.01 MHz). The ¹⁹⁵Pt{¹H} chemical shifts were measured on a Bruker ACP 200 instrument (42.95 MHz) and externally referenced to K₂PtCl₄ in water with downfield chemical shifts reported as positive. NMR spectra were recorded in CDCl₃, unless otherwise stated. The reactions were generally monitored by IR spectroscopy in the ν(CO) region. The isocyanides and alkylating agents were obtained commercially from Alfa Aesar or Aldrich. Dppa and 1,2-bis(2-isocyanophenoxy)ethane were prepared as described in the literature [61].

4.1. Preparation of [(OC)₃Fe(μ-CN-R)(μ-dppa)Pt(PPh₃)] (2)

To a solution of [(CO)₃Fe(μ-CO)(μ-dppa)Pt(PPh₃)] (202 mg, 0.2 mmol) in CH₂Cl₂ (5 ml) was added dropwise one equivalent of the respective isocyanide, dissolved in CH₂Cl₂ (5 ml). After stirring for 20 min. at ambient temperature (CO release), the clear orange-red solution is reduced and the products were precipitated by slow addition of hexane. The yellow to orange-colored products are obtained analytically pure with yields ranging from 75 to 95%.

2c [(OC)₃Fe(μ-CN-Bz)(μ-dppa)Pt(PPh₃)]: Anal. Calcd. for C₅₃H₄₃FeN₂O₃P₃Pt•0.5CH₂Cl₂ (1099.79+42.46): C, 55.68; H, 3.76; N, 2.45. Found: C, 55.77; H, 3.77; N, 2.26 %. IR (CH₂Cl₂): ν(CO) 2002 m, 1934 vs, ν(C=N): 1684 m, br; (KBr) ν(NH) 3276 w, ν(CO) 2001 m, 1933 s, 1920 s, ν(C=N) 1678 m, br cm⁻¹. ¹H NMR: δ = 4.87 (s, 2H, CH₂), 5.00 (m, br, NH, ³J(Pt-H) = 89.2 Hz), 6.56–7.63 (m, 40H, Phenyl).

2d [(CO)₃Fe{μ-CN-CH₂C(=O)OMe}(μ-dppa)Pt(PPh₃)]: Anal. Calcd. for C₄₉H₄₁FeN₂O₅P₃Pt•0.5CH₂Cl₂ (1081.73+42.46): C, 52.89; H, 3.77; N, 2.49. Found: C, 53.01; H, 3.72; N, 2.26 %. IR (CH₂Cl₂): ν(CO) 2006 m, 1940 vs, 1923 sh, ν(C=O) 1750 w, br, ν(C=N) 1676 m, br cm⁻¹. ¹H-NMR: δ = 3.65 (s, 3H, OCH₃), 4.42 (s, 2H, CH₂), 4.97 (m, br, NH, ³J(Pt-H) = 90.0 Hz), 7.06–7.60 (m, 35H, Phenyl).

2e [(CO)₃Fe(μ-CN-CH₂SO₂p-Tol)(μ-dppa)Pt(PPh₃)]: Anal. Calcd. for C₅₄H₄₅FeN₂O₅P₃PtS•1.5CH₂Cl₂ (1177.92+127.39): C, 51.02; H, 3.68; N, 2.14. Found: C, 51.48; H, 3.86; N, 2.37 %. IR (CH₂Cl₂): ν(CO) 2009 m, 1940s, 1922 sh, ν(C=N) 1648 m, br; (KBr) ν(NH)

3250 w, $\nu(\text{CO})$ 1990 m, 1926 s, 1918 s, $\nu(\text{C}=\text{N})$ 1642 m, br cm^{-1} . $^1\text{H NMR}$: $\delta = 2.17$ (s, 3H, CH_3), 4.88 (s, 2H, CH_2), 4.92 (m, br, NH, $^3J(\text{Pt-H}) = 88.2$ Hz), 6.74–7.63 (m, 39H, Aryl).

2f $[(\text{CO})_3\text{Fe}(\mu\text{-CN-Bu-}n)(\mu\text{-dppa})\text{Pt}(\text{PPh}_3)]$: Anal. Calcd. for $\text{C}_{50}\text{H}_{45}\text{FeN}_2\text{O}_3\text{P}_3\text{Pt}\cdot\text{CH}_2\text{Cl}_2$ (1065.77+84.93): C, 53.23; H, 4.18; N, 2.43. Found: C, 53.31; H, 4.41; N, 2.59 %. IR (CH_2Cl_2): $\nu(\text{CO})$: 1988 vs, 1931 vs, $\nu(\text{C}=\text{N})$ 1694 m, br cm^{-1} . $^1\text{H-NMR}$ (243 K): $\delta = 0.64$ –1.57 (m, 9H, Bu), 4.99 (m, br, NH, $^3J(\text{Pt-H}) = 94.0$ Hz), 6.97–7.40 (m, 35H, Phenyl).

2g $[(\text{CO})_3\text{Fe}(\mu\text{-CN-Bu-}tert)(\mu\text{-dppa})\text{Pt}(\text{PPh}_3)]$: Anal. Calcd. for $\text{C}_{50}\text{H}_{45}\text{FeN}_2\text{O}_3\text{P}_3\text{Pt}\cdot 2\text{CH}_2\text{Cl}_2$ (1065.77+169.87): C, 50.55; H, 4.00; N, 2.27. Found: C, 50.36; H, 4.18; N, 2.57 %. IR (KBr): $\nu(\text{NH})$ 3303 w, $\nu(\text{CN})$ 2123 s, $\nu(\text{CO})$: 1950 s, 1909 vs, 1735 m cm^{-1} . $^1\text{H-NMR}$ (263 K): $\delta = 1.25$ (s, 9H, $t\text{Bu}$), 4.98 (m, br, NH, $^3J(\text{Pt-H}) = 89.0$ Hz), 6.90–7.70 (m, 35H, Phenyl).

4.2. Preparation of $[(\text{OC})_2(\text{RNC})\text{Fe}(\mu\text{-CN-R})(\mu\text{-dppa})\text{Pt}(\text{PPh}_3)]$ (**3**):

The preparation was similar to that of series **2** reacting **1** with 2 equivalents of CNR or by reacting **2** with a further equivalent of the respective CNR ligand.

3a $[(\text{OC})_2(\text{xylylNC})\text{Fe}(\mu\text{-CN-xylyl})(\mu\text{-dppa})\text{Pt}(\text{PPh}_3)]$: Anal. Calcd. for $\text{C}_{62}\text{H}_{54}\text{FeN}_3\text{O}_2\text{P}_3\text{Pt}$ (1216.98): C, 61.19; H, 4.47; N, 3.45. Found: C, 61.21; H, 4.55; N, 2.89 %. IR (KBr): $\nu(\text{CO})$ 1943 s, 1908 s, $\nu(\text{CN})$ 2092 m, $\nu(\text{C}=\text{N})$ 1651 m, br cm^{-1} . $^1\text{H-NMR}$: δ 1.82 (s, 6H, Xylyl-Me), 2.09 (s, 6H, Xylyl-Me), 5.27 (m, br, NH, $^3J(\text{Pt-H}) = 101$ Hz), 6.89–7.65 (m, 41H, Aryl).

3b $[(\text{OC})_2(\text{BzNC})\text{Fe}(\mu\text{-CN-Bz})(\mu\text{-dppa})\text{Pt}(\text{PPh}_3)]$: Anal. Calcd. for $\text{C}_{60}\text{H}_{50}\text{FeN}_3\text{O}_2\text{P}_3\text{Pt}\cdot 1.5\text{CH}_2\text{Cl}_2$ (1188.98+127.39): C, 56.12; H, 4.03; N, 3.19. Found: C, 56.79; H, 4.25; N, 3.27 %. IR (CH_2Cl_2): $\nu(\text{CO})$ 1930 s, 1878 s, $\nu(\text{CN})$ 2157 m, $\nu(\text{C}=\text{N})$ 1653 m; (KBr) $\nu(\text{NH})$ 3311w, $\nu(\text{CO})$ 1931 s, 1878 s, $\nu(\text{CN})$ 2157 m, $\nu(\text{C}=\text{N})$ 1652 m cm^{-1} . $^1\text{H-NMR}$: $\delta = 3.69$ (s, 2H, $\text{CH}_2\text{-N}=\text{C}$), 4.89 (s, 2H, $\text{CH}_2\text{-NC}$), 6.75 (m, br, NH, $^3J(\text{Pt-H}) = 89.2$ Hz), 7.01–7.28 (m, 45H, Phenyl).

3c: Anal. Calcd. for $\text{C}_{60}\text{H}_{48}\text{FeN}_3\text{O}_4\text{P}_3\text{Pt}$ (1218.91): C, 59.12; H, 3.97; N, 3.45. Found: C, 59.38; H, 4.12; N, 3.56 %. IR (CH_2Cl_2): $\nu(\text{CO})$ 1953 vs, 1912 s, $\nu(\text{CN})$ 2093 m, $\nu(\text{C}=\text{N})$ 1654 m; (KBr): $\nu(\text{NH})$ 3420 w, $\nu(\text{CO})$ 1948 vs, 1909 s, $\nu(\text{CN})$ 2154 w, 2092 m, $\nu(\text{C}=\text{N})$ 1653 m cm^{-1} . $^1\text{H-NMR}$ (302 K): $\delta = 3.86$ –4.55 (m, br, 4H, $\text{OCH}_2\text{CH}_2\text{O}$), 5.86 (m, br, NH, $^3J(\text{Pt-H}) = 89.2$ Hz), 6.60–7.70 (m, 43H, Aryl).

3d $[(\text{OC})_2(\text{tert-BuNC})\text{Fe}(\mu\text{-CN-xylyl})(\mu\text{-dppa})\text{Pt}(\text{PPh}_3)]$: This very labile product was only characterized in situ by IR spectroscopy and immediately treated with $[\text{Me}_3\text{O}][\text{BF}_4]$ to give stable **5d**. IR (CH_2Cl_2): $\nu(\text{CO})$ 1946 vs, 1899 s, $\nu(\text{CN})$ 2122 m, $\nu(\text{C}=\text{N})$ 1652 m cm^{-1} .

4.3. Preparation of $[(OC)_2(o\text{-anisylNC})Fe(\mu\text{-SO}_2)(\mu\text{-dppa})Pt(PPh_3)]$ (**4**): SO_2 is bubbled for 3 min into a solution of **2b** (111 mg, 0.1 mmol) in CH_2Cl_2 (5 ml). After 10 further min. under SO_2 -atmosphere, the solvent is removed under reduced pressure and the residue recrystallized from CH_2Cl_2/Et_2O . The product has been isolated in form of orange-colored plate-like crystals. Yield: 87 mg; 62%. Anal. Calcd. for $C_{52}H_{43}FeN_2O_5P_3PtS \cdot 0.5CH_2Cl_2$ (1151.84+42.47): C, 52.80; H, 3.71; N, 2.35. Found: C, 53.08; H, 3.84; N, 2.22 %. IR (KBr): $\nu(CN)$ 2125 m, $\nu(CO)$ 1982 s, 1942 s cm^{-1} . 1H NMR: $\delta = 3.49$ (s, 3H, OCH_3), 5.15 (m, br, NH, $^3J(Pt-H) = 92.0$ Hz), 6.60–7.71 (m, 39H, Aryl).

4.4. Preparation of $[(OC)_2(L)Fe\{\mu\text{-CN}(R)R'\}(\mu\text{-dppa})Pt(PPh_3)]^+$ (**5**) :

A solution of the isonitrile complex (0.1 mmol) in CH_2Cl_2 (5 ml) is treated with two equivalents of $[Me_3O][BF_4]$ or $EtOSO_2CF_3$. After stirring for 3-4 h at ambient temperature, all volatiles are removed under reduced pressure and the yellow residue rinsed with ether and then dried under *vacuo*. The yields are almost quantitative. If necessary, recrystallization is done from CH_2Cl_2/Et_2O .

5b $[(OC)_3Fe\{\mu\text{-CN}(Me)Bz\}(\mu\text{-dppa})Pt(PPh_3)][BF_4]$: Anal. Calcd. for $C_{54}H_{46}BF_4FeN_2O_3P_3Pt \cdot 0.5CH_2Cl_2$ (1201.63+42.47): C, 52.62; H, 3.80; N, 2.25. Found: C, 52.58; H, 3.82; N, 2.34 %. IR (CH_2Cl_2): $\nu(CO)$ 2038 m, 1978 vs, $\nu(C=N)$ 1568 m, br; (KBr): $\nu(NH)$ 3216 w, $\nu(CO)$ 2032 m, 1970 vs, 1955 sh, $\nu(CN)$ 1572 w cm^{-1} . 1H NMR: $\delta = 2.61$ (s, 3H, NCH_3), 5.54 (s, 2H, $CH_2\text{-N=C}$), 6.16 (m, br, NH, $^3J(Pt-H) = 92.0$ Hz), 7.15–7.46 (m, 40H, Phenyl).

5c: Anal. Calcd. for $C_{61}H_{51}BF_4FeN_3O_4P_3Pt \cdot Et_2O \cdot CH_2Cl_2$ (1320.75+74.12+84.93): C, 53.57; H, 4.29; N, 2.84. Found: C, 53.68; H, 4.03; N, 3.04 %. IR (KBr): $\nu(NH)$ 3230 w, br, $\nu(CN)$ 2108 s, $\nu(CO)$ 1982 s, 1942 s, $\nu(C=N)$ 1528 w cm^{-1} . 1H NMR: $\delta = 3.01$ (s, 3H, NCH_3), 4.19-4.74 (m, 4H, OCH_2), 5.70 (m, br, NH, $^3J(Pt-H) = 103.0$ Hz), 5.81–7.56 (m, 43H, Aryl). $^{13}C\{^1H\}$ NMR: δ 315.7 (ddd, $\mu\text{-C}$, $^2J(P-C) = 79$, $^2J(P-C) = 16$, $^2J(P-C) = 3$ Hz), 212.9 (dd, 2 $FeCO$, $^2J(P-C) = 25$, $^3J(P-C) = 8$ Hz), 210.5 (d, 1 $FeCO$, $^2J(P-C) = 8$ Hz), 169.4 (dd, $FeCN$, $^2J(P-C) = 30$, $^3J(P-C) = 7$ Hz), 113.9–153.7 (m, Aryl), 68.2 (s, OCH_2), 67.3 (s, OCH_2), 52.4 (m, br, NCH_3).

5d $[(OC)_2(tert\text{-BuNC})Fe\{\mu\text{-CN}(Me)xylyl\}(\mu\text{-dppa})Pt(PPh_3)][BF_4]$: Anal. Calcd. for $C_{59}H_{57}BF_4FeN_3O_2P_3Pt \cdot Et_2O \cdot 0.5CH_2Cl_2$ (1270.80+74.12+42.47): C, 54.97; H, 4.94; N, 3.03 Found: C, 54.98; H, 4.60; N, 2.77 %. IR (KBr): $\nu(NH)$ 3231 w, br, $\nu(CN)$ 2148 s, $\nu(CO)$ 1980 vs, 1937 s, $\nu(C=N)$ 1539 w cm^{-1} . 1H NMR: $\delta = 0.78$ (s, 9H, tBu), 2.22 (s, 3H, Xylyl-Me), 2.37 (s, 3H, Xylyl-Me), 2.85 (s, 3H, NCH_3), 5.98 (m, br, NH, $^3J(Pt-H) = 104.0$ Hz), 7.20–7.86 (m, 38H, Aryl).

5e $[(OC)_3Fe\{\mu\text{-CN}(Me)Bz\}(\mu\text{-dppa})Pt(CNBu\text{-}t)][BF_4]$: Anal. Calcd. for $C_{50}H_{40}BF_4FeN_3O_3P_2Pt$ (1130.57): C, 53.12; H, 3.57; N, 3.72. Found: C, 52.96; H, 3.81; N, 3.42 %. IR (CH_2Cl_2): $\nu(CN)$

2138 s, $\nu(\text{CO})$ 2001 s, 1993 s, 1921 vs, $\nu(\text{C}=\text{N})$ 1568 m, br; (KBr): $\nu(\text{NH})$ 3216 w, $\nu(\text{CO})$ 2032 m, 1970 vs, 1955 sh, $\nu(\text{CN})$ 1577 w cm^{-1} .

5f $[(\text{OC})_3\text{Fe}\{\mu\text{-CN}(\text{Me})\text{xylyl}\}(\mu\text{-dppa})\text{Pt}\{\text{P}(\text{OMe})_3\}][\text{BF}_4]$: To a solution of **5a** (0.1 mmol) in CH_2Cl_2 (5 ml) is added $\text{P}(\text{OMe})_3$ (38 mg, 0.3 mmol) at room temperature. ^{31}P NMR-monitoring of the reaction mixture reveals a quantitative conversion. After 1 h, the yellow solution is reduced to 2 ml and layered with Ether. In the course of several days, yellow crystals are formed at 5°C . Yield: (75 mg, 65%). Anal. Calcd. for $\text{C}_{40}\text{H}_{42}\text{BF}_4\text{FeN}_2\text{O}_6\text{P}_3\text{Pt}\cdot\text{Et}_2\text{O}$ (1077.44 + 74.12): C, 45.89; H, 4.55; N, 2.43%. Found: C, 45.77; H, 4.35; N, 2.20. IR (KBr): $\nu(\text{NH})$ 2830 m, br, 2610 m, br, $\nu(\text{CO})$ 2030m, 1962 vs, $\nu(\text{CN})$ 1557 m cm^{-1} . ^1H -NMR: δ 2.37 (s, 6H, Xylyl-Me), 3.44 (d, 9H, $\text{P}(\text{OMe})_3$, $^3J(\text{P-H}) = 13.0$ Hz), 3.89 (s, NMe), 7.29-8.30 (m, 23H, Aryl), 10.50 (m, br, NH, $^3J(\text{Pt-H}) = 85$ Hz).

5g: Anal. Calcd. for $\text{C}_{48}\text{H}_{45}\text{BF}_4\text{FeN}_4\text{O}_4\text{P}_2\text{Pt}$ (1141.59): C, 50.50; H, 3.97; N, 4.91. Found: C, 50.64; H, 3.83; N, 4.77 %. MS (FAB⁺/NBA-matrix): 1054 M⁺ (25%). IR (CH_2Cl_2): $\nu(\text{CN})$ 2213 m, 2145 vs, $\nu(\text{CO})$ 1990 vs, 1950 s, $\nu(\text{C}=\text{N})$ 1538 w cm^{-1} .

5h and **5h'** $[(\text{OC})_3\text{Fe}\{\mu\text{-CN}(\text{Et})\text{Bz}\}(\mu\text{-dppa})\text{Pt}(\text{PPh}_3)][\text{OSO}_2\text{CF}_3]$: Anal. Calcd. for $\text{C}_{57}\text{H}_{48}\text{F}_3\text{FeN}_2\text{O}_6\text{P}_3\text{PtS}$ (1277.92): C, 52.63; H, 3.78; N, 2.19. Found: C, 52.67; H, 3.78; N, 2.27 %. IR (CH_2Cl_2): $\nu(\text{CO})$ 2036 m, 1976 vs, $\nu(\text{C}=\text{N})$ 1555 w cm^{-1} . **5h** ^1H -NMR: $\delta = 0.37$ (t, 3H, $\text{CH}_2\text{-CH}_3$, $^3J(\text{H-H}) = 7.1$ Hz), 3.13 (q, br, 2H, $\text{CH}_2\text{-CH}_3$, $^3J(\text{H-H}) = 7.1$ Hz), 5.55 (s, 2H, NCH_2), NH signal ND, 7.15–7.46 (m, 40H, Phenyl). **5h'** ^1H -NMR: $\delta = 1.39$ (t, 3H, $\text{CH}_2\text{-CH}_3$, $^3J(\text{H-H}) = 7.1$ Hz), 4.09 (q, br, 2H, $\text{CH}_2\text{-CH}_3$, $^3J(\text{H-H}) = 7.1$ Hz), 4.43 (s, 2H, NCH_2), NH signal ND, 7.15–7.46 (m, 40H, Phenyl).

5i $[(\text{OC})_2(\text{xylylNC})\text{Fe}\{\mu\text{-CN}(\text{Et})\text{xylyl}\}(\mu\text{-dppa})\text{Pt}(\text{PPh}_3)][\text{OSO}_2\text{CF}_3]$: Anal. Calcd. for $\text{C}_{65}\text{H}_{59}\text{F}_3\text{FeN}_3\text{O}_5\text{P}_3\text{PtS}$ (1395.17): C, 55.96; H, 4.26; N, 3.01. Found: C, 55.42; H, 4.10; N, 2.87 %. (FAB⁺/NBA-matrix): 1245 M⁺ (90%), 1189 M⁺ - 2 CO (36%). IR (KBr): $\nu(\text{NH})$ 3240 w, br, $\nu(\text{CN})$ 2121 s, $\nu(\text{CO})$ 1972 vs, 1937 s, $\nu(\text{C}=\text{N})$ 1510 w cm^{-1} . ^1H NMR: $\delta = 0.22$ (t, 3H, $\text{CH}_2\text{-CH}_3$, $^3J(\text{H-H}) = 7.0$ Hz), 1.86 (s, 6H, Xylyl-Me), 1.93 (s, 3H, CH_3), 2.21 (s, 3H, Xylyl-Me), 3.40 (m, br, 1H, $\text{CH}_2^{\text{A}}\text{-CH}_3$), 3.62 (m, br, 1H, $\text{CH}_2^{\text{B}}\text{-CH}_3$), 6.08 (m, 1H, NH, $^3J(\text{Pt-H}) = 102.0$ Hz), 6.75–7.96 (m, 41H, Aryl).

4.5. Preparation of $[(\text{CO})_2\text{LFe}\{\mu\text{-CN}(\text{R}')\text{R}\}(\mu\text{-Ph}_2\text{PNPPH}_2)\text{Pt}(\text{PR}''_3)]$ (**6**)– To a solution of **5** (0.5 mmol) in THF (10 ml) are added 3 mmol KOSiMe_3 or KH. After stirring for 30 min., all volatiles are removed under reduced pressure and the yellow residue extracted with Et_2O (2 x 10 ml). The combined extracts are concentrated and the yellow products precipitated by addition of hexane. After drying *in vacuo*, compounds **6** are obtained in analytical pure form. Yields: 80-95%.

6b [(OC)₃Fe{μ-CN(Me)Bz}(μ-Ph₂PNPPh₂)Pt(PPh₃)]: Anal. Calcd. for C₅₄H₄₅FeN₂O₃P₃Pt (1113.82): C, 58.23; H, 4.07; N, 2.52%. Found: C, 58.18; H, 4.25; N, 2.37. IR (KBr): ν(CO) 1996 m, 1936 vs, 1922 s, ν(CN) 1550 m cm⁻¹. ¹H NMR: δ = 2.40 (s, 3H, NCH₃), 5.41 (s, 2H, CH₂-N=C), 7.08–7.87 (m, 40H, Phenyl).

6c [(OC)₃Fe{μ-CN(Me)xylyl}(μ-Ph₂PNPPh₂)Pt(CNBu-*t*)]: To a solution of **6a** (113 mg, 0.1 mmol) in 4 ml of CH₂Cl₂ were added via microsyringe 4 eq. of CNBu-*t*. After stirring for 30 min., the solution was reduced to 1 ml. After addition of 5 ml of hexane a yellowish powder precipitated, which was dried under *vacuo*. **6c** was characterized only spectroscopically. IR (KBr): ν(CO) 2010 m, 1940 vs, ν(CN) 2190 s cm⁻¹. ¹H NMR: δ 1.46 (s, 9H, *t*-Bu), 2.18 (s, 6H, Xylyl-Me), 7.10-7.78 (m, 23H, Aryl).

6d [(OC)₃Fe{μ-CN(Me)xylyl}(μ-Ph₂PNPPh₂)Pt{P(OMe)₃}] : Anal. Calcd. for C₄₀H₄₁FeN₂O₆P₃Pt (989.63): C, 48.55; H, 4.18; N, 2.83%. Found: C, 48.90; H, 4.37; N, 2.60. IR (KBr): ν(CO) 2006 m, 1937 vs, ν(CN) 1533 m cm⁻¹. ¹H NMR: δ 2.21 (s, 6H, Xylyl-Me), 3.40 (d, 9H, P(OCH₃), ³J(P-H) = 13.2 Hz), 3.66 (s, NMe), 7.11-7.82 (m, 23H, Aryl).

6e [(OC)₂(xylylNC)Fe{μ-CN(Et)xylyl}(μ-Ph₂PNPPh₂)Pt(PPh₃)]: Anal. Calcd. for C₆₄H₅₈FeN₃O₂P₃Pt•0.5CH₂Cl₂ (1244.74 + 42.47): C, 60.17; H, 4.62; N, 3.26%. Found: C, 60.33; H, 5.09; N, 3.21. IR (KBr): ν(CN) 2097 s, ν(CO) 1956 vs, 1922 s, ν(CN) 1587 w cm⁻¹. ¹H-NMR: δ 0.16 (t, 3H, CH₂-CH₃, ³J(H-H) = 7.0), 1.69 (s, 6H, Xylyl-Me), 1.94 (s, 3H, Xylyl-Me), 2.31 (s, 3H, Xylyl-Me), 3.28 (m, br, 1H, CH₂^A-CH₃), 3.48 (m, br, 1H, CH₂^B-CH₃), 6.74-7.86 (m, 41H, Aryl).

4.6. *Preparation of [(CO)₂LFe{μ-CN(R')R}{μ-Ph₂PN(Me)PPh₂}Pt(PPh₃)] (7)* – A solution of **6** (0.2 mmol) in CH₂Cl₂ (6 ml) is treated with an excess of CH₃I and stirred for 6 h in the dark. After reduction of the volume to 3 ml, the yellow product is precipitated by addition of Et₂O and dried in *vacuo*. Yields: 70-72%.

7a and **7a'** [(OC)₃Fe{μ-CN(Me)Bz}{μ-Ph₂PN(Me)PPh₂}Pt(PPh₃)]**[I]**: Anal. Calcd. for C₅₅H₄₈FeIN₂O₃P₃Pt (1255.76): C, 52.61; H, 3.85; N, 2.23%. Found: C, 52.79; H, 3.72; N, 2.35. IR (KBr): ν(CO) 2034 m, 1970 vs, ν(CN) 1571 m cm⁻¹. (FAB⁺/NBA-Matrix): 1129 M⁺ (78%), 1101 M⁺ - CO (38%). **7a** ¹H-NMR: δ = 2.40 (d, 3H, P₂NCH₃, ³J(P-H) = 4.9 Hz), 2.58 (s, 3H, NCH₃), 5.47 (s, 2H, CH₂-N=C), 6.31–7.59 (m, 40H, Phenyl). **7a'** ¹H-NMR: δ = 2.40 (d, 3H, P₂NCH₃, ³J(P-H) = 4.9 Hz), 3.71 (s, 3H, NCH₃), 4.39 (s, 2H, CH₂-N=C), 6.31–7.59 (m, 40H, Phenyl).

7b [(OC)₂(xylylNC)Fe{μ-CN(Et)xylyl}{μ-Ph₂PN(Me)PPh₂}Pt(PPh₃)]**[I]**: Anal. Calcd. for C₆₅H₆₁FeIN₃O₂P₃Pt (1386.98): C, 56.29; H, 4.43; N, 3.03%. Found: C, 56.65; H, 4.82; N, 2.85. IR (KBr): ν(CN) 2126 s, ν(CO) 1980 vs, 1945 s, ν(CN) 1516 m cm⁻¹. ¹H NMR: δ 0.28 (t, 3H, CH₂-

CH_3 , $^3J(H-H) = 7.0$ Hz), 1.33 (s, 3H, Xylyl-Me), 2.03 (s, 6H, Xylyl-Me), 2.28 (s, 3H, Xylyl-Me), 2.45 (t, 3H, NMe, $^3J(P-H) = 6.1$ Hz) 3.21 (m, 1H, $CH_2^A-CH_3$), 3.64 (m, 1H, $CH_2^B-CH_3$), 6.84-7.79 (m, 41H, Aryl).

4.7. Preparation of $[(OC)_3Fe\{\mu-CN(Me)xylyl\}\{\mu-Ph_2PN(AuPPh_3)PPh_2\}Pt(PPh_3)][OSO_2CF_3]$ (**8a**)

A solution of $[AuClPPh_3]$ (109 mg, 0.22 mmol) in CH_2Cl_2 (6 ml) is reacted with an equivalent amount of silver triflate and then filtered after 2h. After addition of **6a** (226 mg, 0.2 mmol) and stirring for 1h, the solution is layered with Et_2O . During the course of several days, yellow crystals of **8a** are formed. Yield: (211 mg, 58%). Anal. Calcd. for $C_{74}H_{62}AuF_3FeN_2O_6P_4PtS \cdot CH_2Cl_2$ (1736.17 + 84.93): C, 49.47; H, 3.54; N, 1.54%. Found: C, 50.00; H, 3.91; N, 1.40. IR (KBr): $\nu(CO)$ 2021 m, 1962s vs, 1942 sh, $\nu(CN)$ 1544 w cm^{-1} . 1H NMR: δ 2.31 (s, 6H, Xylyl-Me), 2.85 (s, 3H, NMe), 6.81-7.51 (m, 53H, Aryl).

4.8. Preparation of $[(OC)_2(xylyl)NC]Fe\{\mu-CN(Et)xylyl\}\{\mu-Ph_2PN(AuPPh_3)PPh_2\}Pt(PPh_3)][OSO_2CF_3]$ (**8b**) – This compound was prepared in a similar manner. Yield: (233 mg, 60%). Anal. Calcd. for $C_{83}H_{73}AuF_3FeN_3O_5P_4PtS \cdot CH_2Cl_2$ (1853.37 + 84.93): C, 52.05; H, 3.90; N, 2.17%. Found.: C, 51.81; H, 3.96; N, 1.90. IR (KBr): $\nu(CN)$ 2115 s, $\nu(CO)$ 1971 vs, 1936 vs, $\nu(CN)$ 1509 w cm^{-1} . 1H -NMR: δ 0.28 (t, 3H, CH_2-CH_3 , $^3J(H-H) = 7.1$), 1.95 (s, 6H, Xylyl-Me), 2.00 (s, 3H, Xylyl-Me), 2.41 (s, 3H, Xylyl-Me), 3.41 (m, 1H, $CH_2^A-CH_3$), 3.56 (m, 1H, $CH_2^B-CH_3$), 6.79-7.89 (m, 56H, Aryl).

4.9. Preparation of $[(OC)_3Fe\{\mu-CN(Me)xylyl\}\{\mu-Ph_2PN(CuAsPh_3)PPh_2\}Pt(PPh_3)][OSO_2CF_3]$ (**8c**)

– To a solution of **6a** (226 mg, 0.2 mmol) in CH_2Cl_2 (6 ml) is added an equivalent amount of $[Cu(AsPh_3)_3][NO_3]$. After 1h the solution is filtered, layered with Et_2O and kept in a refrigerator. In the course of several days, yellow crystals of **8c** are formed. Yield: (185 mg, 51%). Anal. Calcd. for $C_{73}H_{62}AsCuFeN_3O_6P_3Pt \cdot CH_2Cl_2$ (1736.17 + 84.93): C, 54.04; H, 3.93; N, 2.56%. Found: C, 53.21; H, 4.26; N, 2.94. IR (KBr): $\nu(CO)$ 2013 m, 1950s vs, br $\nu(CN)$ 1543 w cm^{-1} . 1H NMR: δ 2.31 (s, 6H, Xylyl-Me), 2.82 (s, 3H, NMe), 6.91-7.54 (m, 53H, Aryl).

4.10. Preparation of $[(OC)_3Fe\{\mu-CN(Me)xylyl\}\{\mu-Ph_2PN(HgMe)PPh_2\}Pt(PPh_3)]Cl$ (**8e**) -

To a solution of **6a** (113 mg, 0.1 mmol) in CH_2Cl_2 (5 ml) is added $MeHgCl$. After 1h the solution is filtered, layered with Et_2O and kept in a refrigerator. In the course of several hours, yellowish **8e** precipitates. Yield: (211 mg, 43%). Anal. Calcd. for $C_{56}H_{62}HgClFeN_2O_3P_3Pt$ (1391.01): C, 48.47; H, 3.35; N, 2.01%. Found: C, 49.00; H, 3.11; N, 1.90. IR (KBr): $\nu(CO)$ 2021 m, 1962s vs, 1942

sh, $\nu(\text{CN})$ 1544 w cm^{-1} . $^1\text{H NMR}$: δ 0.99 (s, 3H, $^2J(^{199}\text{Hg-H}) = 204.5$ Hz), 2.19 (s, 6H, Xylyl-Me), 2.76 (s, 3H, NMe), 6.71-7.58 (m, 38H, Aryl)

4.11. *Preparation of* $[(\text{OC})_3\text{Fe}\{\mu\text{-CN}(\text{Et})\text{xylyl}\}\{\mu\text{-Ph}_2\text{PN}(\text{HgMe})\text{PPh}_2\}\text{Pt}(\text{PPh}_3)][\text{Cl}]$ (**8f**). This compound was prepared in a similar manner by addition of MeHgCl to a CH_2Cl_2 solution of **6e**. Anal. Calcd. for $\text{C}_{65}\text{H}_{61}\text{ClHgFeN}_3\text{O}_2\text{P}_3\text{Pt}$ (1496.11): C, 52.18; H, 4.11; N, 2.81%. Found: C, 51.76; H, 3.81; N, 2.60. IR (CH_2Cl_2): $\nu(\text{CN})$ 2121 s, $\nu(\text{CO})$ 1977 vs, 1942 s cm^{-1} . $^1\text{H NMR}$: δ 0.30 (t, 3H, $\text{CH}_2\text{-CH}_3$, $^3J(\text{H-H}) = 7.2$), 0.92 (s, 3H, $^2J(^{199}\text{Hg-H}) = 202.0$ Hz), 1.88 (s, 6H, Xylyl-Me), 1.95 (s, 3H, Xylyl-Me), 2.30 (s, 3H, Xylyl-Me), 3.32 (m, 1H, $\text{CH}_2^{\text{A}}\text{-CH}_3$), 3.62 (m, 1H, $\text{CH}_2^{\text{B}}\text{-CH}_3$), 6.80-7.88 (m, 41H, Aryl).

4.12. Crystal structure determinations

Data of **5d** and **8b** were collected on a Siemens Stoe AED2 diffractometer using graphite-monochromated Mo $\text{K}\alpha$ radiation ($\lambda = 0.71073$ Å). The intensities were collected using $\Omega/2\theta$ scans, and the intensities of three standard reflections, which were measured after every 90 min, remained stable throughout the data collection. The intensities were corrected for Lorentz and polarization effects. An empirical absorption correction based on the Ψ -scans of three reflections was employed. Data of **3b** and **5b** were collected on a Stoe IPDS diffractometer using graphite-monochromated Mo $\text{K}\alpha$ radiation ($\lambda = 0.71069$ Å). The intensities were determined and corrected by the program INTEGRATE in IPDS (Stoe & Cie, 1999). An empirical absorption correction was employed using the FACEIT-program in IPDS (Stoe & Cie, 1999). Data of **2c** and **8a** were collected on a Oxford Diffraction Xcalibur S diffractometer with graphite-monochromated Mo- $\text{K}\alpha$ radiation ($\lambda = 0.71073$ Å). The built in programs were used for data collection (CrysAlis CCD) and cell refinement, data reduction and multi-scan absorption correction (CrysAlis RED) [62]. The structures were generally solved by direct and Fourier methods using SHELXS-90 [63]. For each structure, the non-hydrogen atoms were refined anisotropically. The H-atoms were placed in geometrically calculated positions and fixed to isotropic displacement parameters based on a riding-model except for the NH atom in **2c**, which was refined independently. Refinement of the structures was carried out by full-matrix least-squares methods based on F_o^2 using SHELXL-97 [63]. In the crystal of **8a** the triflate anion is disordered, but only one position was refined. The crystallographic data for each complex are gathered in Table 5 and S1. CCDC 1031960 (**2c**), 1031961 (**3b**), 1031962 (**5b**), 1031963 (**5d**), 1031964 (**8a**), contain further supplementary crystallographic data for this paper. These data can be obtained free of charge from The Cambridge Crystallographic Data Centre via www.ccdc.cam.ac.uk/data_request/cif.

Acknowledgements

We are grateful to the *Deutsche Forschungsgemeinschaft* and the *CNRS* for financial support.

Appendix A. Supplementary material

Supplementary material related to this article can be found online at <http://doi:>

ACCEPTED MANUSCRIPT

References

- [1] (a) R.J. Puddephatt, *Chem. Soc. Rev.*, 12 (1983) 99–127;
(b) B. Chaudret, B. Delavaux, R. Poilblanc, *Coord. Chem. Rev.* 86 (1988) 191–243;
(c) J.T. Mague, *J. Cluster Sci.* 6 (1995) 217–269.
- [2] M.S. Balakrishna, V.S. Reddy, S.S. Krishnamurty, J.F. Nixon, J.C.T.R. Burckett St. Laurent, *Coord. Chem. Rev.* 129 (1994) 1–90.
- [3] A. Blagg, G.R. Cooper, P.G. Pringle, R. Robson, B.L. Shaw, *J. Chem. Soc. Chem. Commun.* (1984) 933–934.
- [4] R. Uson, J. Fornies, R. Navarro, J.I. Cebollada, *J. Organomet. Chem.* 304 (1986) 381–390.
- [5] (a) M. Knorr, P. Braunstein, A. Tiripicchio, F. Ugozzoli, *J. Organomet. Chem.* 526 (1996) 105–16;
(b) F. Balegroune, P. Braunstein, J. Durand, T. Faure, D. Grandjean, M. Knorr, M. Lanfranchi, C. Massera, X. Morise, A. Tiripicchio, *Monatshefte Chem.* 132 (2001) 885–896;
(c) P. Braunstein, J. Durand, M. Knorr, C. Strohmann, *Chem. Commun.* (2001) 211–212.
- [6] Y. Yang, L. McElwee-White, *Dalton Trans.* (2004) 2352–2356.
- [7] I. Jourdain, M. Knorr, C. Strohmann, C. Unkelbach, S. Rojo, P. Gomez-Iglesias, F. Villafane, *Organometallics* 32 (2013) 5343–5359.
- [8] (a) N. Nawar, *J. Organomet. Chem.* 590 (1999) 217–221;
(b) N. Nawar, *J. Organomet. Chem.* 605 (2000) 1–6.
- [10] S. Todisco, V. Gallo, P. Mastrorilli, M. Latronico, N. Re, F. Creati, P. Braunstein, *Inorg. Chem.* 51 (2012) 11549–11561.
- [11] M. Knorr, C. Strohmann, *Europ. J. Inorg. Chem.* (1998) 495–499.
- [12] K.K. Joshi, O.S. Mills, P.L. Pauson, B.W. Shaw, W.H. Stubbs, *Chem. Commun.* (1965) 181–182.
- [13] (a) R.D. Adams, F.A. Cotton, J.M. Troup, *Inorg. Chem.* 13 (1974) 257–262;
(b) R.D. Adams, F.A. Cotton, *Inorg. Chem.* 13 (1974) 249–253.
- [14] I. Jourdain, L. Vieille-Petit, S. Clément, M. Knorr, F. Villafañe, C. Strohmann, *Inorg. Chem. Commun.* 9 (2006) 127–131.
- [15] P.S. Braterman, *Metal Carbonyl Spectra*, Academic Press, London, New York, 1975.
- [16] J.A.S. Howell, J.-Y. Saillard, A. Le Beuze, G. Jouen, *J. Chem. Soc. Dalton Trans.* (1982) 2533–2537.
- [17] K.R. Grundy, K.N. Robertson, *Organometallics* 2 (1983) 1736–1742.
- [18] J. Wu, M.K. Reinking, P.E. Fanwick, C.P. Kubiak, *Inorg. Chem.* 26 (1987) 247–252.
- [19] S.T. Belt, S.B. Duckett, D.M. Haddleton, R.N. Perutz, *Organometallics* 8 (1989) 748–759.
- [20] K.S. Ratliff, P.E. Fanwick, C.P. Kubiak, *Polyhedron* 9 (1990) 2651–2653.
- [21] S. Clément, S.M. Aly, D. Bellows, D. Fortin, C. Strohmann, L. Guyard, A.S. Abd-El-Aziz, M. Knorr, P.D. Harvey, *Inorg. Chem.* 48 (2009) 4118–4133.
- [22] W.A. Schenk, *Angew. Chem.* 26 (1987) 98–109.
- [23] (a) O. Heyke, G. Beuter, I.P. Lorenz, *Z. Naturforsch.* 47B (1992) 668–674;
(b) M. Knorr, C. Strohmann, *Organometallics* 18 (1999) 248–257;

- see also: (c) A. F. Bartlone, M.F. Chetcuti, R. Navarro, M. Shang, *Inorg. Chem.* 34 (1995) 980–983;
- (d) W.A. Schenk, *Z. Naturforsch.* 41B (1986) 663–664.
- [24] G. Cox, C. Dowling, A.R. Manning, P. McArdle, D. Cunningham, *J. Organomet. Chem.* 438 (1992) 143–158.
- [25] V.G. Albano, L. Busetto, M.C. Cassani, P. Sabatino, A. Schmitz, V. Zanotti, *J. Chem. Soc. Dalton Trans.* (1995) 2087–2093.
- [26] D.L. DeLaet, P.E. Fanwick, C.P. Kubiak, *Organometallics* 5 (1986) 1807–1811.
- [27] A. Schröder, W. Sperber, J. Fuchs, W.P. Fehlhammer, *Chem. Ber.* 125 (1992) 1101–1105.
- [28] T. Mayer, H.-C. Böttcher, *Polyhedron* 69 (2014) 240–243.
- [29] (a) C.S. Browning, D.H. Farrar, D.C. Frankel, J.J. Vittal, *Inorg. Chim. Acta* 254 (1997) 329–338;
(b) C.S. Browning, D.H. Farrar, *J. Chem. Soc., Dalton Trans.* (1995) 521–530.
- [30] J. Ellermann, P. Gabold, F.A. Knoch, M. Moll, D. Pohl, J. Sutter, W. Bauer, *J. Organomet. Chem.* (1996) 89–107.
- [31] For other examples of hydrogen bonding in dppa complexes see: R. Ahuja, M. Nethaji, A.G. Samuelson, *Polyhedron* 26 (2007) 142–148.
- [32] J.A.S. Howell, P. Mathur, *J. Chem. Soc. Dalton Trans.* (1982) 43–50.
- [33] H.-W. Frühauf, D. Meyer, J. Breuer, *J. Organomet. Chem.* 297 (1985) 211–228.
- [34] M.J. Chetcuti, K.J. Deck, J.C. Gordon, B.E. Grant, P.E. Fanwick, *Organometallics* 11 (1992) 2128–2139.
- [35] H. Knoll, H. Hennig, B. Walther, H.-C. Böttcher, D.J. Stufkens, *Inorg. Chim. Acta* 210 (1993) 33–37.
- [36] S.M. Breckenridge, N.J. Taylor, A.J. Carty, *Organometallics* 10 (1991) 837–840.
- [37] S. Doherty, M.R.J. Elsegood, W. Clegg, M.F. Ward, M. Waugh, *Organometallics* 16 (1997) 4251–4253.
- [38] M.R. Churchill, K.M. Keil, T.S. Janik, M.C. Willoughby, *J. Coord. Chem.* 52 (2001) 229–244.
- [39] P.J. Low, A.J. Carty, K.A. Udachin, G.D. Enright, *Chem. Commun.* (2001) 411–412.
- [40] D. Taher, H. Pritzkow, B. Walfort, H. Lang, *J. Organomet. Chem.* 691 (2006) 793–798.
- [41] T. Kremer, F. Hampel, F.A. Knoch, W. Bauer, A. Schmidt, P. Gabold, M. Schütz, J. Ellermann, P.v.R. Schleyer, *Organometallics* 15 (1996) 4776–4782.
- [42] M.T. Gamer, M. Rastatter, P.W. Roesky, *Z. Anorg. Allg. Chem.* 628 (2002) 2269–2272.
- [43] T. Li, J. Jenter, P.W. Roesky, *Z. Anorg. Allg. Chem.* 636 (2010) 2148–2155.
- [44] J. Geicke, I.P. Lorenz, P. Märtschel, K. Polborn, *Z. Naturforsch. B* 52 (1997) 593–603.
- [45] M. Haehnel, S. Hansen, A. Spannenberg, P. Arndt, T. Beweries, U. Rosenthal, *Chem. Eur. J.* 18 (2012) 10546–10553.
- [46] (a) D. Pohl, J. Ellermann, F.A. Koch, M. Moll, *J. Organomet. Chem.* 481, (1994) 259–274;
(b) I. Bachert, I. Bartussek, P. Braunstein, E. Guillon, J. Rosé, G. Kickelbick, *J. Organomet. Chem.* 580, (1999) 144–151.
- [47] (a) J. Ellermann, W. Wend, *Z. Anorg. Allg. Chem.* 543 (1986) 169–185;

- (b) J. Ellermann, W. Wend, *Nouv. J. Chim.* 10 (1986) 313–318.
- [48] A.P. Bella, O. Crespo, J.E. Fernandez, A.K. Fischer, P.G. Jones, A. Laguna, J.M. Lopez-de-Luzuriaga, M. Monge, *J. Chem. Soc. Dalton Trans.* (1999) 4009–4017.
- [49] (a) J. Braddock-Wilking, L.-B. Gao, N. P. Rath, *Dalton Trans.* 39 (2010) 9321–9328;
(b) P.D. Harvey, W.P. Schaefer, H.B. Gray, *Inorg. Chem.* 27 (1988) 1101–1104;
(c) C.-H. Tao, V.W.-W. Yam, *J. Photochem. Photobiology C: Photochemistry Reviews* 10 (2009) 130–140;
(d) V. Pawlowski, H. Kunkely, C. Lennartz, K. Böhn, A. Vogler, *Eur. J. Inorg. Chem.* (2004) 4242–4246;
(e) J.A.G. Williams, *Photochemistry and Photophysics of Coordination Compounds: Platinum*, in: V. Balzani, S. Campagna (Eds.) *Photochemistry and Photophysics of Coordination Compounds II*, Springer Berlin Heidelberg, 2007, pp. 205–268.
- [50] (a) C. King, M.N.I. Khan, R. J. Staples, J.P. Fackler, Jr., *Inorg. Chem.* 31 (1992) 3236–3238;
(b) T.L. Stott, M.O. Wolf, B.O. Patrick, *Inorg. Chem.* 44 (2005) 620–627;
(c) V.W.-W. Yam, E.C.-C. Cheng, *Photochemistry and Photophysics of Coordination Compounds: Gold*, in: V. Balzani, S. Campagna (Eds.) *Photochemistry and Photophysics of Coordination Compounds II*, Springer Berlin Heidelberg, 2007, pp. 269–309.
- [51] P.D. Harvey, H.B. Gray, *J. Am. Chem. Soc.* 110 (1988) 2145–2147.
- [52] D.P. Sergers, M.K. DeArmond, P.A. Grutsch, C. Kutal, *Inorg. Chem.* 23 (1984) 2874–2878.
- [53] (a) A. Díez, J. Forniés, A. Garcia, E. Lalinde, M.T. Moreno, *Inorg. Chem.* 44 (2005) 2443–2453;
(b) A. Lapprand, N. Khiri, D. Fortin, S. Jugé, P. D. Harvey, *Inorg. Chem.* 52 5 (2013) 2361–2371.
- [54] (a) G. Steyl, *Acta Cryst. Section E* 65 (2009) m272;
(b) G.A. Bowmaker, R.D. Hart, E.N. De Silva, B.W. Skelton, A.H. White, *Aust. J. Chem.* 50 (1997) 553–565.
- [55] N. Burford, B.W. Royan, R.E.V.H. Spence, T.S. Cameron, A. Linden, R.D. Rogers, *J. Chem. Soc. Dalton Trans* (1990) 1521–1528.
- [56] V.V. Sushev, A.N. Kornev, Y.V. Fedotova, Y.A. Kursky, T.G. Mushtina, G.A. Abakumov, L.N. Zakharov, A.L. Rheingold, *J. Organomet. Chem.* 676 (2003) 89–93.
- [57] A successful argentation of dppa has been reported: R. Uson, A. Laguna, M. Laguna, M.a.C. Gimeno, P.G. Jones, C. Fittschen, G.M. Sheldrick, *J. Chem. Soc., Chem. Commun.* (1986) 509–510.
- [58] The reaction of [(THF)₃LiN(PPh₂)₂Ni(COD)] with Me₃SnCl is reported to give [Me₃SnN(PPh₂)₂Ni(COD)]: M. Said, D.L. Hughes, M. Bochmann, *Polyhedron* (2006) 843–852.
- [59] W.S. Sheldrick, P. Bell, *Inorg. Chim. Acta* 137 (1987) 181–188.
- [60] (a) L. Busetto, M. Salmi, S. Zacchini, V. Zanotti, *J. Organomet. Chem.* 693 (2008) 57–67;
(b) L. Busetto, R. Mazzoni, M. Salmi, S. Zacchini, V. Zanotti, *J. Organomet. Chem.* 695 (2010) 2519–2525.
- [61] (a) H. Nöth, L. Meinel, *Z. Anorg. Allgem. Chem.* 349 (1967) 225–240;
(b) R. J. Angelici, M. H. Quick, G. A. Kraus, D. T. Plummer, *Inorg. Chem.* 21 (1982) 2178–2184.
- [62] CrysAlis CCD, CrysAlis RED and CrysAlis PRO, Oxford Diffraction Ltd, Abingdon (UK) 2012.

[63] (a) G.M. Sheldrick, SHELX-97, Program for the Solution of Crystal Structures, University of Göttingen, Göttingen, Germany, 1997; (b) G. M. Sheldrick, Acta Cryst. (2008) A64 112-122.

ACCEPTED MANUSCRIPT

Synthesis and Reactivity of Bis(diphenylphosphino)amine-bridged Heterobimetallic Iron-Platinum μ -Isonitrile and μ -Aminocarbonyl Complexes

Michael Knorr* [a], Isabelle Jourdain* [a], Ahmed Said Mohamed, [a] Abderrahim Khatyr [a], Stephan Koller [b], Carsten Strohmann [b]

^a*Institut UTINAM UMR CNRS 6213, Université de Franche-Comté, Faculté des Sciences et des Techniques, 16, Route de Gray, 25030 Besançon, France*

^b*Institut für Anorganische Chemie der Technischen Universität Dortmund, Otto-Hahn-Strasse 6, 44227 Dortmund, Germany*

Table of Content

Fig. S1. Perspective view of 2c showing the atom-labelling scheme.	Page S2
Fig. S2. ¹ H NMR spectra at variable temperature of complex 3a in CDCl ₃ .	Page S3
Fig. S3. ³¹ P{ ¹ H} NMR spectrum of complex 5g in CDCl ₃ at 298 K.	Page S4
Fig. S4. ³¹ P{ ¹ H} NMR spectrum of complex 5f in CDCl ₃ at 298 K.	Page S4
Fig. S5. ¹⁹⁵ Pt{ ¹ H} NMR spectrum showing the isomers 7a and 7a' in CDCl ₃ at 298 K.	Page S5
Fig. S6. ¹⁹⁵ Pt{ ¹ H} NMR spectrum of heterotrimetallic complex 8b in CDCl ₃ at 298 K.	Page S5
Fig. S7. Perspective view of cation of 8b showing the atom-labelling scheme.	Page S6
Fig. S8. Normalized absorption (blue) and emission (red) spectra of 5a recorded in CH ₂ Cl ₂ at 298 K and in the solid state at 298 K.	Page S7
Fig. S9. Emission of 8a in 2-MeTHF.	Page S7
Table S1. Crystallographic and refinement data for 2c and 8b .	Page S8

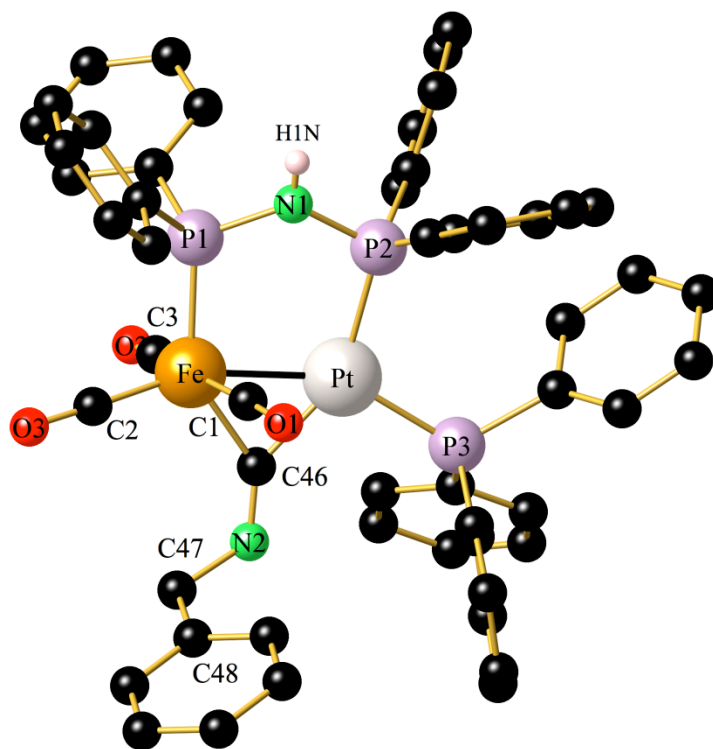


Fig. S1. Perspective view of **2c** showing the atom-labelling scheme. Hydrogen atoms and the CH_2Cl_2 molecule have been omitted for clarity. Selected distances (\AA) and angles ($^\circ$): Fe–Pt 2.5425(4), Fe–P(1) 2.2087(8), Pt–P(2) 2.2924(7), Pt–P(3) 2.2550(7), Fe–C(1) 1.795(3), Fe–C(2) 1.758(3), Fe–C(3) 1.790(3), Fe–C(46) 2.023(3), Pt–C(46) 1.993(3), C(46)–N(2) 1.233(3), C(47)–N(2) 1.465(3), C(1)–O(1) 1.141(3), C(2)–O(3) 1.150(4), C(3)–O(2) 1.139(4), P(1)–N(1) 1.689(2), P(2)–N(1) 1.699(2); P(1)–Fe–Pt 93.29(2), P(2)–Pt–Fe 97.952(19), P(3)–Pt–Fe 152.322(19), P(3)–Pt–P(2) 109.64(2), Pt–C(46)–Fe 78.55(10), C(1)–Fe–Pt 74.94(9), C(2)–Fe–Pt 159.76(9), C(3)–Fe–Pt 91.83(10), C(46)–Pt–P(3) 101.44(8), C(46)–Pt–P(2) 147.89(8), C(46)–Fe–P(1) 143.08(8), N(2)–C(46)–Fe 139.8(2), N(2)–C(46)–Pt 140.9(2), C(46)–N(2)–C(47) 122.2(2), P(1)–N(1)–P(2) 123.10(15).

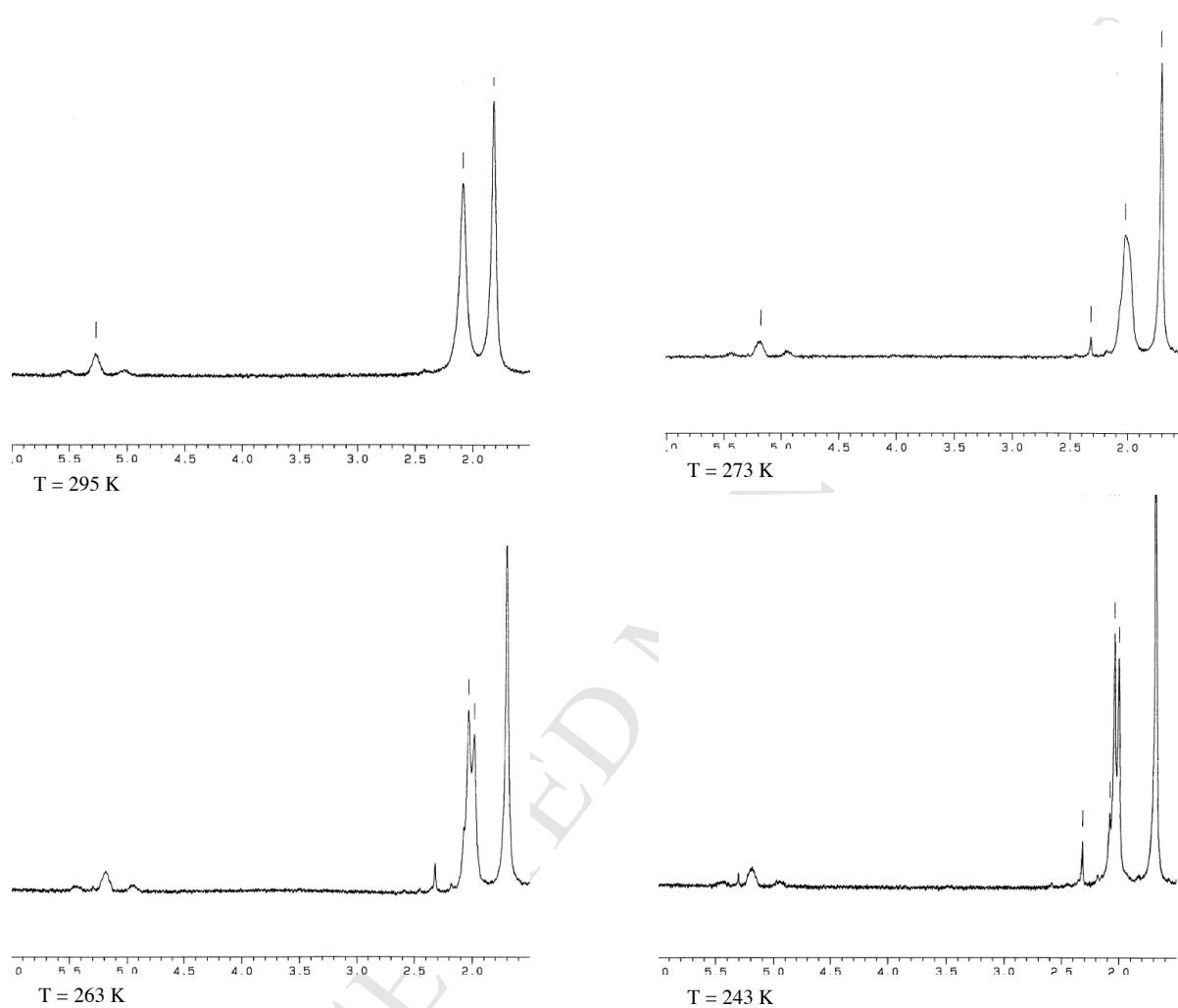


Fig. S2. ^1H NMR spectra at variable temperature of complex **3a** in CDCl_3

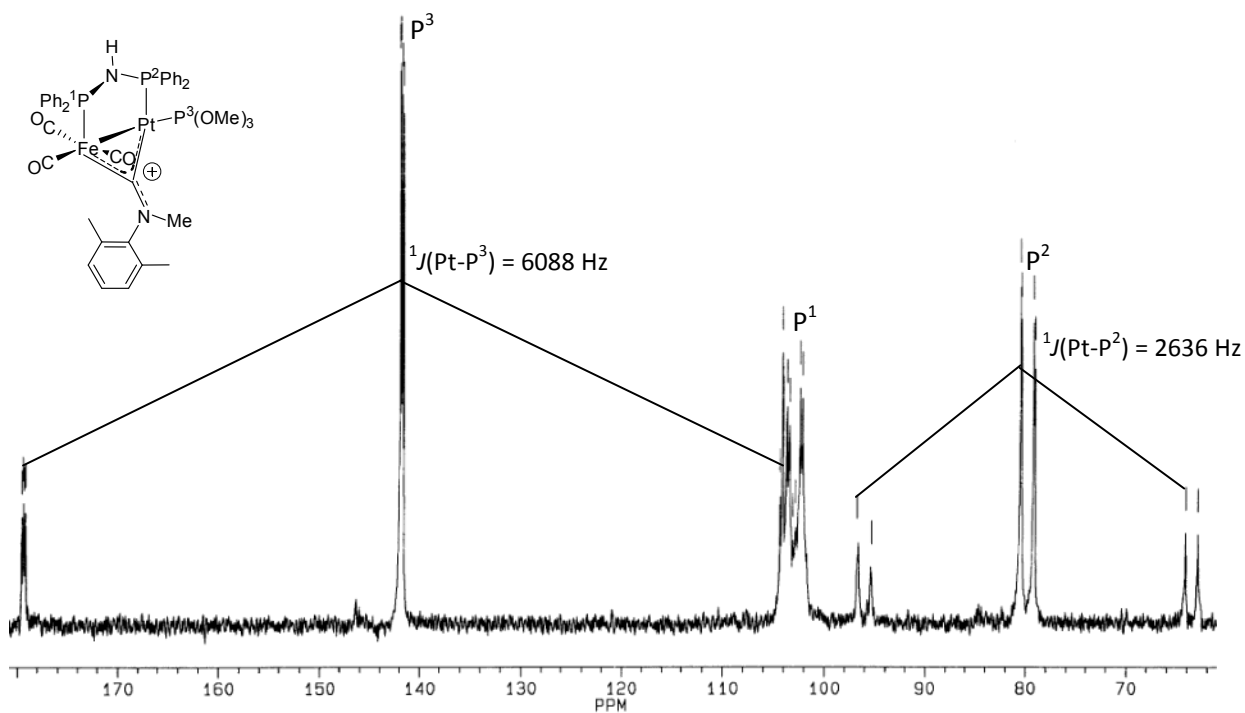


Fig. S4. $^{31}\text{P}\{^1\text{H}\}$ NMR spectrum of complex **5f** in CDCl_3 at 298 K

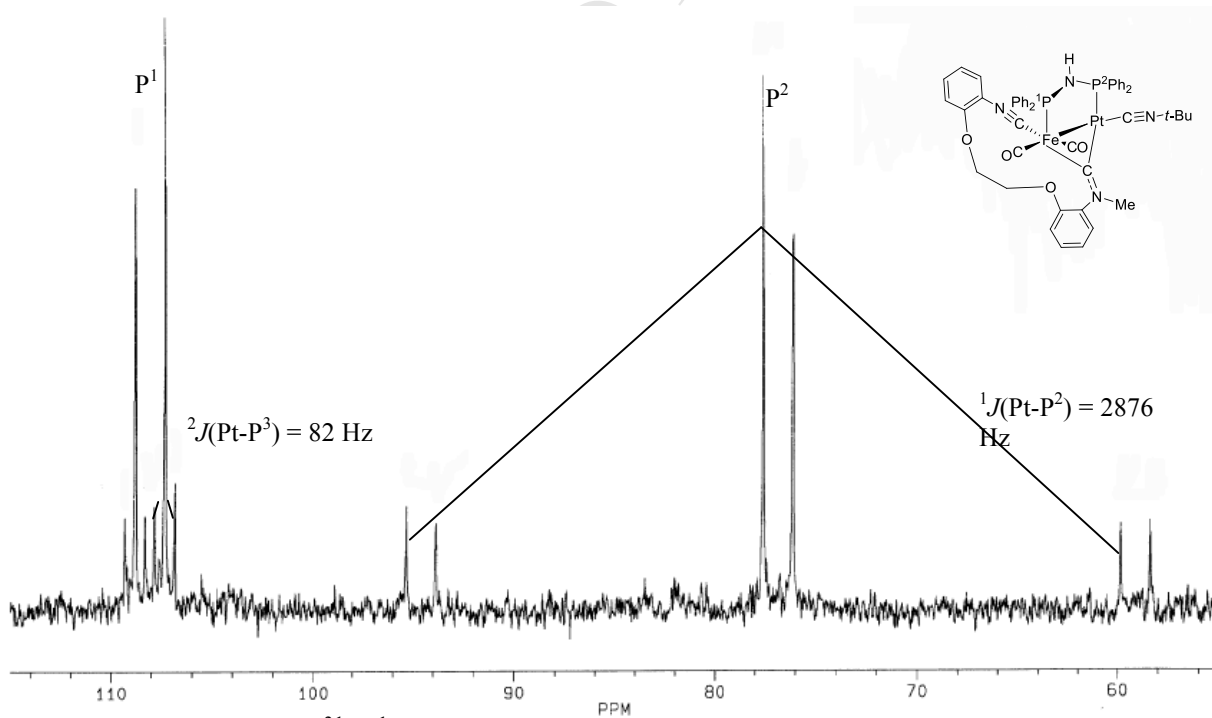


Fig. S3. $^{31}\text{P}\{^1\text{H}\}$ NMR spectrum of complex **5g** in CDCl_3 at 298 K

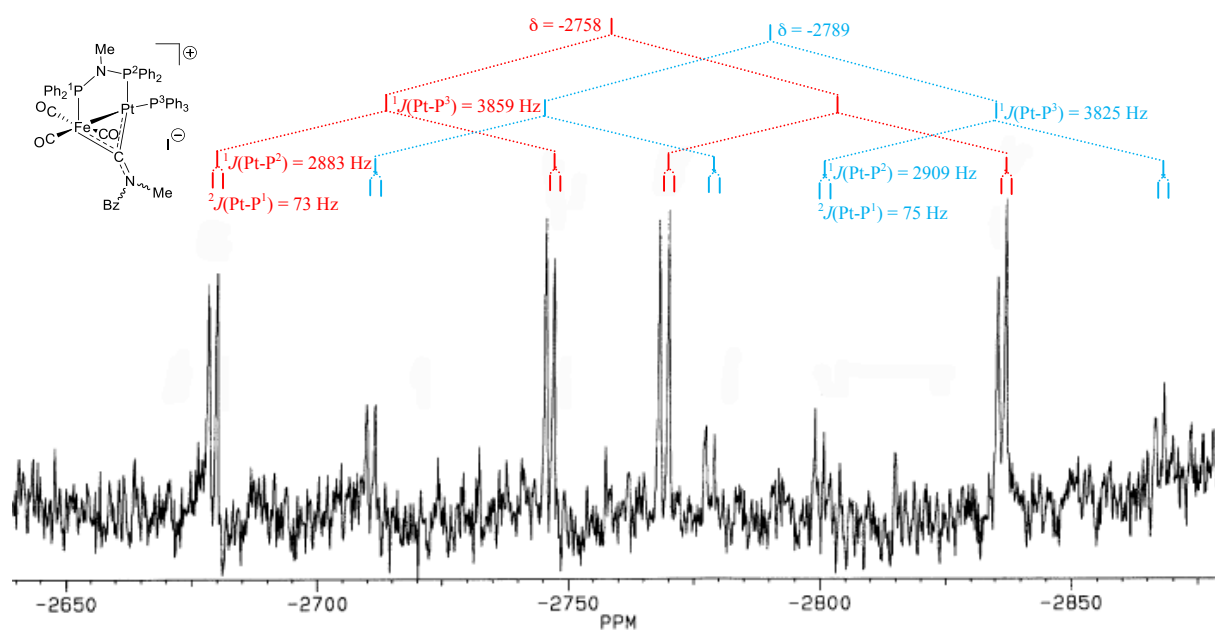


Fig. S5. ¹⁹⁵Pt{¹H} NMR spectrum showing the isomers **7a** and **7a'** in CDCl₃ at 298 K

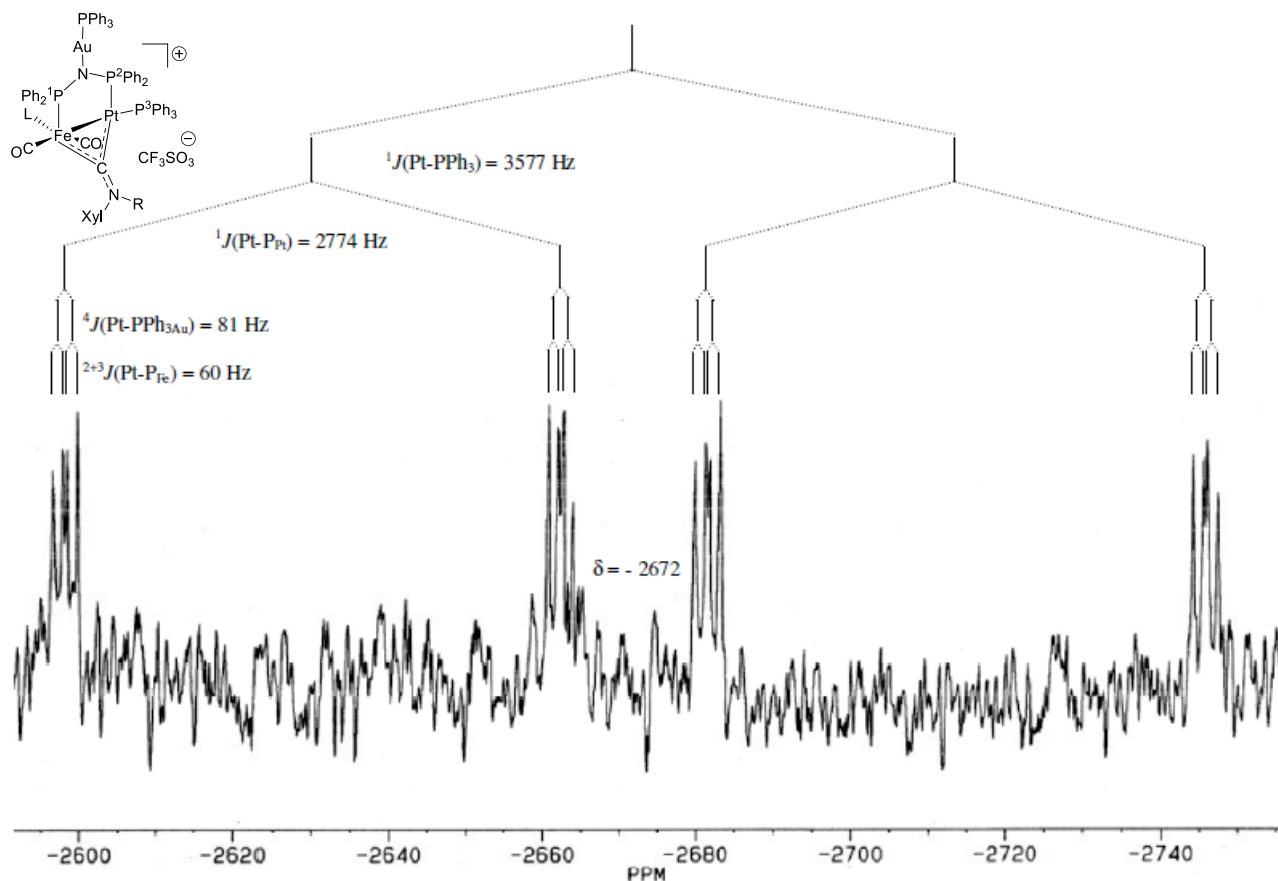


Fig. S6. ¹⁹⁵Pt{¹H} NMR spectrum of heterotrimeric complex **8b** in CDCl₃ at 298 K.

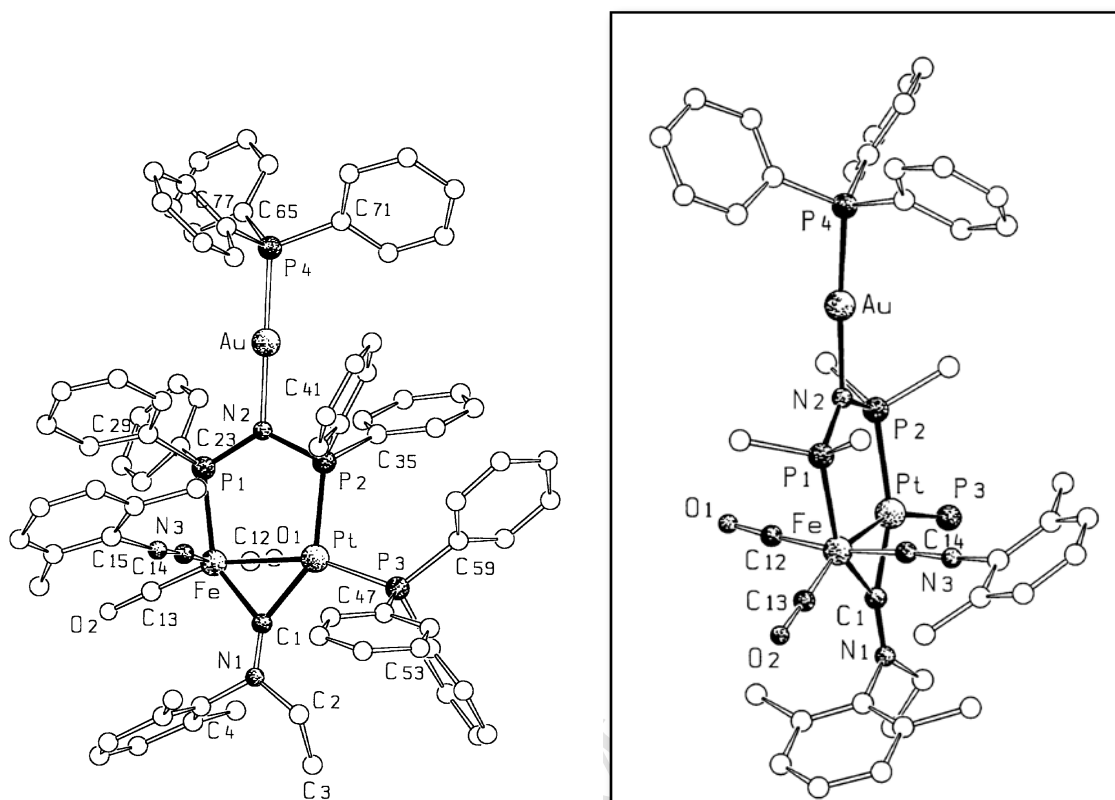


Fig. S7. Perspective view of cation of **8b** showing the atom-labelling scheme. Selected distances (Å) and angles (°): Fe–Pt 2.4943(13), Fe–P(1) 2.237(2), Pt–P(2) 2.282(2), Pt–P(3) 2.271(2), Fe–C(12) 1.750(11), Fe–C(13) 1.761(11), Fe–C(14) 1.823(11), Fe–C(1) 1.912(8), Pt–C(1) 1.967(8), C(1)–N(1) 1.278(10), C(2)–N(1) 1.483(11), P(2)–N(2) 1.672(6), P(1)–N(2) 1.655(7), Au–N(2) 2.060(6), Au–P(4) 2.215(2); P(1)–Fe–Pt 95.83(7), P(2)–Pt–Fe 94.87(6), P(3)–Pt–Fe 158.34(7), P(2)–Pt–P(3) 106.32(8), Pt–C(1)–Fe 80.0(3), Pt–Fe–C(12) 80.8(3), Pt–Fe–C(13) 159.0(3), Pt–Fe–C(14) 93.5(3), C(1)–Pt–P(3) 109.7(3), C(1)–Pt–P(2) 143.9(2), C(1)–Fe–P(1) 146.6(2), N(1)–C(1)–Fe 134.7(6), P(1)–N(2)–P(2) 122.6(4), N(2)–Au–P(4) 176.2(2).

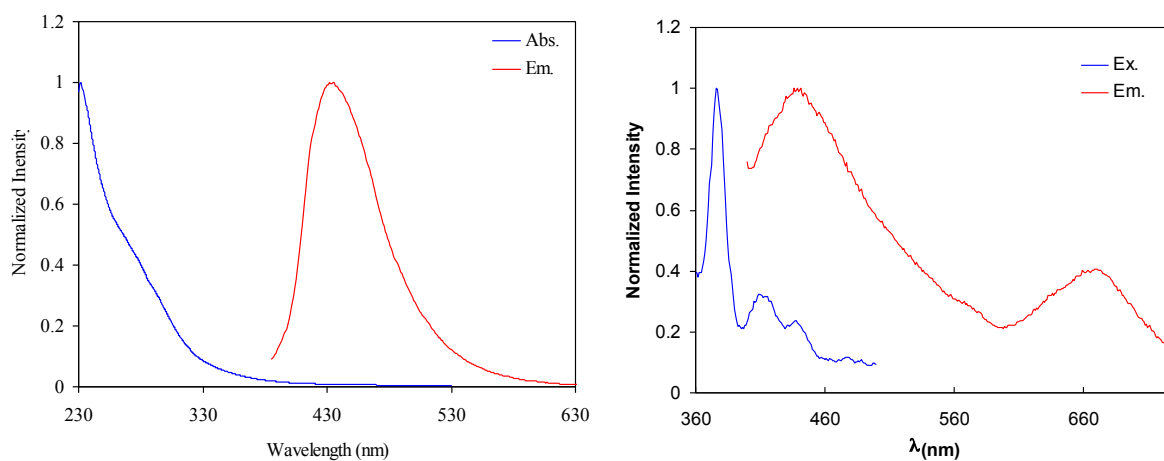


Fig. S8. Normalized absorption (blue) and emission (red) spectra of **5a** recorded in CH₂Cl₂ at 298K (left) and in the solid state at 298 K (right).

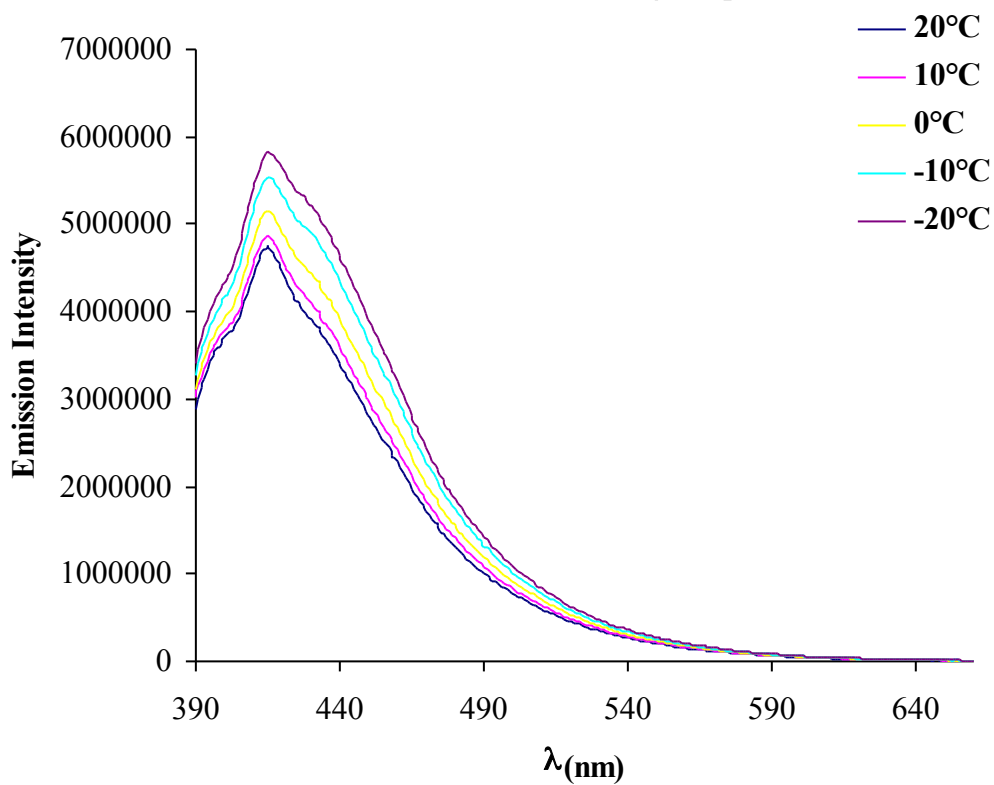


Fig. S9. Emission of **8a** in 2-MeTHF

Table S1. Crystallographic and refinement data for **2c** and **8b**.

	2c •CH ₂ Cl ₂	8b •CH ₂ Cl ₂
CCDC number	1031960	
Formula	C ₅₄ H ₄₅ Cl ₂ FeN ₂ O ₃ P ₃ Pt	C ₇₄ H ₆₂ AuF ₃ FeN ₂ O ₆ P ₄ PtS
Formula weight [g·mol ⁻¹]	1184.67	1736.10
T [K]	173(2)	173(2)
Crystal size [mm]	0.30 x 0.20 x 0.10	0.30 x 0.20 x 0.10
Crystal system	monoclinic	monoclinic
Space group	P2 ₁ /n (14)	P2 ₁ /n (14)
a [Å]	11.4361(2)	16.8304(5)
b [Å]	25.7364(5)	20.7199(4)
c [Å]	17.3652(4)	21.38066(6)
α [°]	90	90
β [°]	106.295(2)	109.644(3)
γ [°]	90	90
V [Å ³]	4905.68(18)	7162.0(3)
Z	4	4
ρ calc [g·cm ⁻³]	1.604	1.610
μ [mm ⁻¹]	3.397	4.370
F (000)	2360	3416
θ range [°]	2.44 – 27.00	2.20 – 27.00
	-14 ≤ h ≤ 14	-21 ≤ h ≤ 21
Index ranges	-32 ≤ k ≤ 32	-26 ≤ k ≤ 26
	-22 ≤ l ≤ 22	-27 ≤ l ≤ 27
collected reflections	93476	79775
independent reflections	10702 (R _{int} = 0.0453)	15595
Data / Restraints / Parameters	10702 / 0 / 599	15595 / 0 / 836
Goodness-of-fit on F ²	1.036	1.064
largest diff peak and hole [e Å ⁻³]	0.947 and -1.086	2.759 and -1.238
final R indices [I > 2σ(I)]	R1 = 0.0236 wR2 = 0.0498	R1 = 0.0325, wR2 = 0.0657
R indices (all data)	R1 = 0.0308 wR2 = 0.0526	R1 = 0.0587 wR2 = 0.0679